ACE Deliverable 2.4-D7

Structuring Research on Conformal Antennas: Final Report

Project Number: FP6-IST 508009
Project Title: Antenna Centre of Excellence
Document Type: Deliverable

Document Number: FP6-IST 508009/ 2.4-D7
Contractual date of delivery: December 31, 2005
Actual Date of Delivery: December 30, 2005
Workpackage: 2.4-3 Structuring Research on Conformal Antennas
Estimated Person Months: 16
Security (PP,PE,RE,CO): PP
Nature: Deliverable Report
Total Number of Pages: 68
File name-revision: ACE-A2.4D7.pdf (Rev. 2)
Organisation responsible for this deliverable: Chalmers University of Technology
Editor(s): Zvonimir Sipus
Participants: KUL, Alcatel, TAS, TUD, DLR, UKARL, POLITO, UNISI, CHALMERS, EMW, KTH, TNO.

Abstract

The basic objective of this workpackage is to better structure the on-going research on conformal antennas, dispersed in several European universities or industrial Research centres. The document describes the following actions: (a) Description of advantages and critical items for various conformal antennas, together with comparison of conformal antennas and corresponding planar antennas. Although some activities were previously made in this direction, the systematic study of these questions was not achieved till now. (b) Description of selected benchmarking structures, suitable as validation cases for most-interesting types of conformal antennas. For three geometries the benchmarking simulations are compared with measurements. (c) Report on the developed hybrid spectral domain-UTD method, which is a result of joining research activities of different groups. The basic idea behind the developed hybrid method is to combine different analysis methods for conformal antennas (the spectral domain method and the UTD in particular) and, at the same time preserving the advantages of each considered method. (d) Description of the Ph.D. course on planar and conformal microstrip antennas that will be held at EPFL- Lausanne in February 2006. This course will cover the theoretical aspect of the analysis and design of planar and conformal antennas.

Keyword List

antenna arrays, conformal antennas, conformal arrays, benchmarking structures, antenna array mutual coupling, numerical methods, hybrid analysis methods, diffraction theory, spectral-domain method, education

European Commission - 6th Framework Programme	***ACE (Antenna Centre of Excellence)***	Information Society Technologies

ACE WP 2.4-3
Structuring Research on Conformal Antennas
Deliverable 2.4-D7
Final Report

Institution	**Authors**
Chalmers Tekniska Högskola AB	Zvonimir Sipus (Editor)
Technische Universität Darmstadt	Jens Freese
Deutsches Zentrum für Luft- und Raumfahrt e.V.	Michael Thiel
Università degli Studi di Siena	Antonio Pippi
Ericsson Microwave Systems	Maria Lanne
Kungliga Tekniska Högskolan	Patrik Persson
Netherlands Organisation for Applied Scientific Research – TNO	Roland Bolt

Document Evolution		
Revision	Date	Status
Rev. 1	07/12/2005	First spread issue
Rev. 2	30/12/2005	Final version of the report

Table of contents

1 INTRODUCTION

This document represents the Deliverable 2.4-D7: Final report of the ACE WP 2.4-3 “Structuring Research on Conformal Antennas”. The document describes advantages and critical items for various conformal antennas, describes selected benchmarking structures that will be used for validating different programs for analysing conformal antennas, describes a developed hybrid program for analysing conformal arrays, and give the description of the Ph.D. course on conformal antennas.

A conformal antenna is defined as an antenna which conforms to a surface whose shape is mainly determined by considerations other than electromagnetic, e.g. aerodynamic or hydrodynamic considerations. This definition should be extended with antennas whose shape is not planar and whose shape is determined with specific electromagnetic reasons like coverage requirements. For example, arrays on cylindrical structures offer a possibility either to create directed beams in arbitrary direction in horizontal plane, or to create an omnidirectional pattern. Spherical arrays have the capability of directing single or multiple beams through a complete hemisphere.

1.1 Description of Work – ACE WP 2.4-3

For convenience, we will repeat the objectives and the description of work that was given in the Technical Annex [1]:

The basic objective is to better structure the on-going research on conformal antennas, dispersed in several European universities or industrial Research centres. In more in details:

- make an inventory of the on-going research,
- sum-up advantages and critical items for various conformal antennas:
  - *from* single or a few thin elements integrated on a car structure, or a cylinder (for base-stations)
  - *to* sophisticate “smart skins” on aircrafts, acting as multi-function arrays merging radar, altimeter and communication missions
- provide specific inputs for activity 1.1 concerning modelling tools, which should apply also to conformal antennas;
- structure continued research in direction of the most useful antenna architectures & geometries, and help students/Ph.D exchange between various European academies and companies.

The description of the planned activities is:

- Inventory of on-going research in Europe.
- Select conformal geometries of interest for future relevant Communication and Radar systems.
- Contribute to activity 1.1 (modelling methods and software), for all aspects specific to conformal antennas. Propose validation cases, launch benchmarking simulations, and compare results with measurements.
- Structure future research by planning complementary Ph.D’s, and submitting common proposals for Research Projects to the European Commission and other relevant public Agencies in Europe.

The current deliverable is:

- 2.4-D7: Final report of the ACE WP 2.4-3 “Structuring Research on Conformal Antennas”.

The document describes the following actions:

- Description of advantages and critical items for various conformal antennas, together with comparison of conformal antennas and corresponding planar antennas. Although some activities were previously made in this direction, the systematic study of these questions was not achieved till now.
- Description of selected benchmarking structures, suitable as validation cases for most-interesting types of conformal antennas. Furthermore, for three geometries the benchmarking simulations are compared with measurements. This activity is done together with the activity 1.1 (modelling methods and software).
- Report on the developed hybrid spectral domain-UTD method. The developed method is a result of structuring research in direction of the most useful antenna architectures & geometries. One of the activities was to join research activities of different groups. The basic idea behind the hybrid method is to combine different analysis methods for conformal antennas (the spectral domain method and the UTD in particular) and, at the same time preserving the advantages of each considered method.
- Description of the Ph.D. course on planar and conformal microstrip antennas that will be held at EPFL- Lausanne in February 2006. This course will cover the theoretical aspect of the analysis and design of planar and conformal antennas. The conformal part of the course will cover low and high frequency analysis methods, as well as practical aspects of designing conformal arrays. The lecturers will be experts from EPFL, KUL, Chalmers, Ericsson and KTH.

This report is continuation of the deliverable 2.4-D6 where the inventory of on-going research in Europe was given.

1.2 Participants

The participating entities in this work package are the following ones (reference numbers as in the Consortium Agreement and Technical Annex [1]):

No.	Organisation	Short Name	Country
2	Katholieke Universiteit Leuven	KUL	Belgium
7	Alcatel Space	Alcatel	France
10	Thales Airborne Systems	TAS	France
14	Technische Universität Darmstadt	TUD	Germany
15	Deutsches Zentrum für Luft- und Raumfahrt e.V.	DLR	Germany
17	Universität Karlsruhe	UKARL	Germany
20	Politecnico di Torino	POLITO	Italy
23	Università degli Studi di Siena	UNISI	Italy
29	Chalmers Tekniska Högskola AB	CHALMERS	Sweden
30	Ericsson Microwave Systems	EMW	Sweden
32	Kungliga Tekniska Högskolan	KTH	Sweden
36	Netherlands Organisation for Applied Scientific Research – TNO	TNO	The Netherlands

Participating organisations.

2 CONFORMAL ANTENNAS: A COMPARISON OF VARIOUS ANTENNA ARRAY GEOMETRIES

Patrik Persson, *KTH*
Jens Freese, *TUD*

2.1 Introduction

The rapid growth in wireless communications, especially mobile communications, has caused the requirements on antenna systems to be more and more demanding. For example, future antenna systems will have a variety of beam forming and beam steering capabilities, and they will be integrated in the surfaces of different vehicles or platforms. For example, a modern aircraft has many antennas protruding from the structure, for navigation, various communication systems, instrument landing systems, radar altimeter etc, as shown in Figure 2.1-A. There can be as many as 20 different antennas or more (up to 70 antennas on a typical military aircraft has been quoted [1]), causing considerable drag and increased fuel consumption. Integrating these antennas into the aircraft skin is highly desirable [2]. Preferably some of the antenna functions should be combined in the same unit if the design can be made broadband enough.

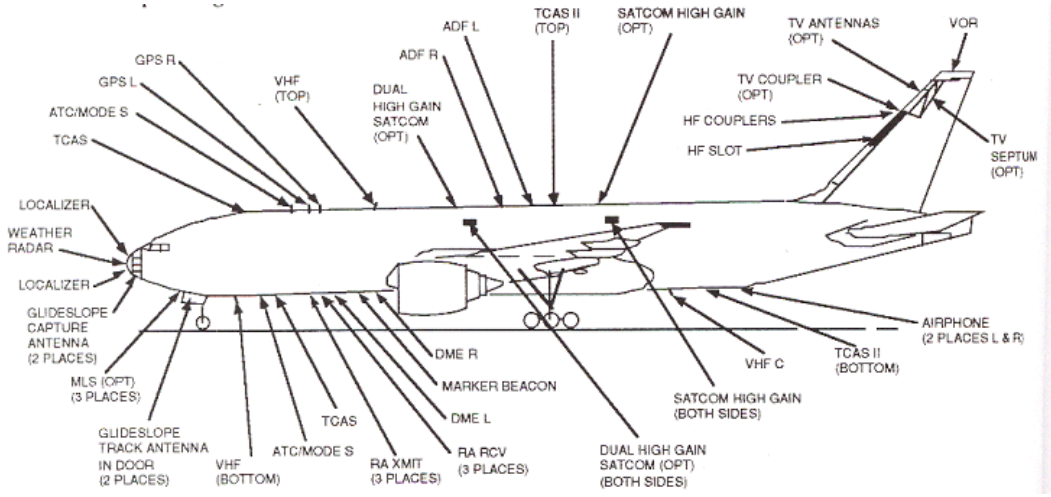

Figure 2.1-A: At least 20-30 antennas protrude from the skin of a modern aircraft [3].

The need for such antennas, conformal antennas, is even more pronounced for the large sized apertures that are necessary for functions like satellite communication and military airborne surveillance radars. In order to ensure proper operation of the communication systems, it is important to be able to determine the characteristics of these antennas.

An indication of a recent resurge in the interest in conformal antennas is the series of Conformal Antenna Workshops, held in Europe every second year, starting from 1999. The first four were held in Karlsruhe (Germany), The Hague (The Netherlands), Bonn (Germany), and Stockholm (Sweden), with the fifth scheduled for Bristol (UK) in 2007.

In this report we will sum up advantages and critical items for various conformal antennas, and make comparisons of conformal antennas and corresponding planar antennas. Furthermore, conformal geometries of interest for future relevant communication and radar systems will be discussed. A more thorough overview of the theory and design of conformal array antennas is found in [4].

2.2 Conformal arrays versus planar arrays

The most obvious difference between a conformal array and a planar array is the geometry and the grid lattice. In the planar case the elements are typically located in a symmetric rectangular or triangular grid. Thus, the planar array can in most applications be analyzed as an infinite array and there are known methods for this [13] (special techniques may need to be applied for the edge elements). The planar array should also be simpler and cheaper to manufacture.

But in some applications the aerodynamics is of great importance. A planar array does not always fulfil this requirement, and a aerodynamically shaped radome may be necessary. Take the nose radar in an aircraft as an example. The radar is flat and it is covered with a radome, i.e. there is a lot of wasted space behind the radome. In addition, the space that the radome occupies around the periphery of the array may limit the array diameter.

The operational bandwidth and maximum scan angle of planar arrays have fundamental limitations. If elements are placed much closer than half a wavelength the mutual coupling will increase and the antenna performance may be degraded. However, due to the element size there is always a lower limit for the spacing. If they are placed further apart, the maximum scan angle is limited by grating lobes. For a conformal array an active sector can be moved along the surface. Thus, the scan angle is increased and the grating lobe phenomenon is reduced. This presumes that the elements can be turned on and off during operation. Otherwise, “conformal grating lobes” may appear from the elements pointing in the wrong direction.

Furthermore, arrays on cylindrical structures offer a possibility either to create directed beams in arbitrary direction in horizontal plane, or to create an omnidirectional pattern. Spherical arrays have capability of directing single or multiple beams through the complete hemisphere.

Another advantage with a conformal array is the radar cross section which in many cases will be lower than for a planar array. When a plane wave is incident on a curved surface the energy will be diffracted along the surface and the reflected energy will be defocused and hence have lower intensity compared with the reflection from a planar surface.

The arguments for and against conformal arrays can be discussed at length. The applications and requirements are quite variable, leading to different conclusions. In spite of this, and to encourage further discussions, we present a summary in Table 2.2-A.

Parameter	**Planar Array**	**Conformal Array**
Technology	Mature	Not fully established
Analysis tools	Available	In development
Beam control	Phase only usually sufficient, fixed amplitude	Amplitude and phase, more complicated
Polarization	Single can be used (dual often desired)	Polarization control required, esp. if doubly curved
Gain	Drops with increased scan	Controlled, depends on shape
Frequency bandwidth	Typically 20 %	Wider than planar is possible
Angular coverage	Limited to roughly $\pm$ 60°	Very wide, half sphere
RCS	Large specular RCS	Lower than planar
Installation on platform	Planar shape limits due to swept volume	Structurally integrated, leaves extra space. No drag.
Radome	Aberration effects	No conventional radome, no boresight error
Packaging of electronics	Known multilayer solutions	Size restriction if large curvature, facets possible

Table 2.2-A: Planar vs. conformal array antennas [4].

2.3 Array Shape Selection and Optimization

When discussing possible conformal antennas for the future, one interesting feature is the shape of the antenna. Of course the shape depends a lot on the platform and finally, in the design process, it will determine the final shape of the antenna. In this case the optimization of the element positions within the array is an important task to achieve a desired angular coverage with a given antenna gain, angular resolution, etc., with a minimum amount of hardware [4], [6].

However, in the first place it is of interest to study the general properties of the antenna characteristics vs. the shape of the antenna. The following Table 2.3-A is partly taken from [7] and indicates the coverage required and the possible shape of the associated antenna relating to various military and civil applications. The table shows that many applications could utilise non-planar antennas with benefits to platform installation in some cases and to angular coverage in other cases.

Role	Nominal Coverage		Array Shape
	Azimuth	Elevation	
Airborne Early Warning & Surface Surveillance	+30° to +150°	-70° to 70°	Cylindrical sector along fuselag
Airborne Intercept	-100° to +100°	-70° to 120°	a) "Ogival" along radome b) Hemispherical inside radome c) Conical inside radome
Terrain Following and Avoidance	-45° to +45°	-60 to +20	Following shape of leading edge of wing
Ground Mapping by Synthetic Aperture, Ground Moving-Target indication	+45° to +135°	-60° to +10°	Cylindrical sector (horizontal axis) a) pod in manned aircraft b) conformal in UAV
Short Range Anti-Surface Targets	360°	-50° to +50°	Cylinder mounted on helicopter mast (vertical axis)
Naval Multi-Function Air Defence	360°	-20° to 90°	Cylinder or conical frustum around mast (vertical axis)
Ground Based Air Defence	360°	-5° to +80°	Conical frustum around mast (vertical axis)
Battlefield Surveillance	360°	-20° to +20°	Cylinder (vertical axis)
SatCom in Mobile Terminals	360°	-10° to +90°	Spherical sector
Base station with SDMA capability	e.g. 120° or 360°	-10° to 0°	Cylindrical sector or cylinder

Table 2.3-A: Potential military and civil applications: Required coverage and possible array shapes, partly from [7].

In [8] a performance rating of the different antenna shapes is made on the basis of the minimum effective antenna area over the coverage region. The total number of radiating elements required is taken as a measure of cost. The ratio of the two is taken as a quality index (performance/cost) for comparison purposes. Note, the effective antenna area A_{eff} is approximately equal to the projected area in the scan direction; it is assumed to vary as $(\cos\theta_s)^{\alpha}$, where $\alpha > 1$ accounts for mismatch loss and θ_s is the (local) scan angle. However, we have for simplicity chosen to present results only for the ideal case $\alpha = 1$. Furthermore, the number of elements required to cover the total antenna surface is denoted A_{tot} and is used as a measure of cost.

The studied shapes differ in curvature and in the slope on the sides. This is important in the trade-off of performance versus scan angle. The focus here is on the minimum effective area within the scan region, but in reality, the requirements are often more detailed and different weights can be given to different regions of the coverage.

A summary of how different shapes make use of the available size ($2R=D$ base diameter) is shown in Figure 2.3-A, where the planar case is included for reference. All cases shown (except the pyramid and the plane) have $h/D=0.5$. We see that performance very much depends on the antenna shape. The pyramid makes poor use of the available base area (inscribed in the $2R$ diameter circle). The plane surface performs well up to the scan limit of 60°, but covers only 50 % of the required volume [8].

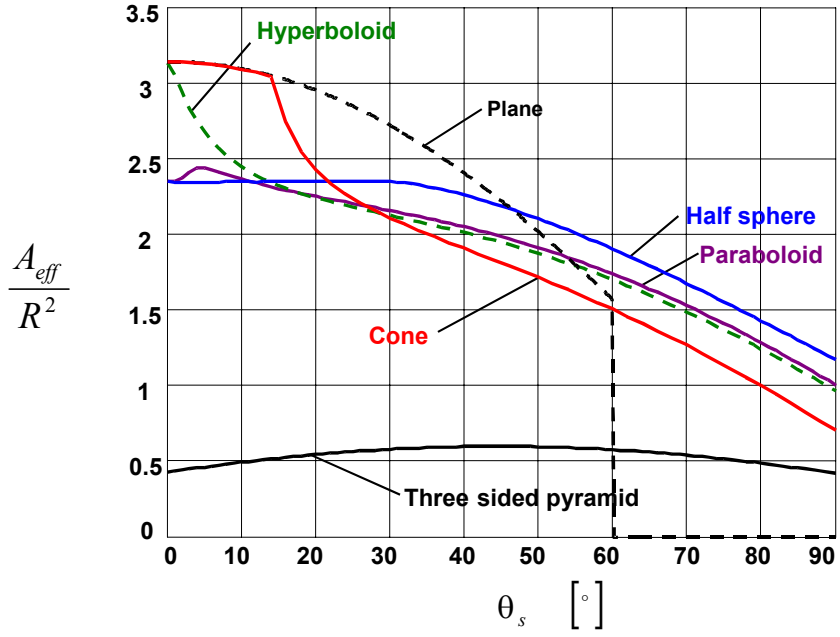

Figure 2.3-A: The effective area for several types of surfaces [8].

The effective area versus total area is summarized for several shapes in Figure 2.3-B. The maximum and minimum effective areas within the scan region are indicated. It is of course desirable to obtain a large effective area with a shape that has a small total area, thus solutions in the upper part and to the left are the very best. The closed cylinder is an extreme case with a very large total area (both the top planar and the curved sides are used here), thus high cost. It performs marginally better than the hyperboloid but has twice the total area. The half sphere is also relatively expensive. The variations with scan angle were illustrated in Figure 2.3-A. Conical shapes come out favorably in this comparison. A further advantage with cones is the constant slope of the surface, possibly simplifying a physical realization [8].

It should be remembered that the presented results are based on a geometrical analysis, not including electromagnetic aspects, impedance variations, pattern performance, polarization effects etc. It is clear that specific application requirements may lead to other shapes optimized not for maximum effective antenna area, as was assumed here, but optimized for some other criterion. For instance, it has been found that a pyramidal arrangement with five to six surfaces (one pointing upwards) can be optimum depending on what system requirements are most important [9]. It has also been shown that six surfaces can be the best alternative when the impact on system noise temperature is of main concern [10].

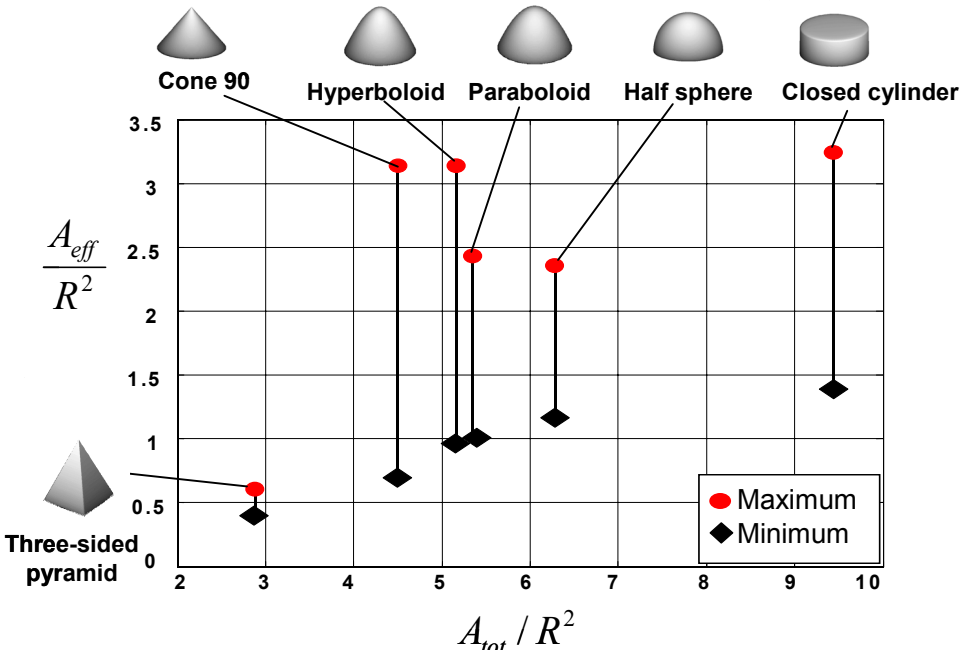

Figure 2.3-B: Maximum and minimum values of the effective antenna area vs. the total antenna area for several conformal antenna shapes [8].

However, based on the chosen criteria to maximize the effective antenna area within the scan region, in [8] it was found that curved solutions in general exhibit much better performance than solutions based on planar surfaces. This is, in fact, true for both the two-dimensional and three-dimensional cases.

2.4 Electromagnetic and Beamforming Considerations

In previous sections an overview is given on what to expect from conformal array antennas when compared with planar antennas. However, to fully understand the characteristics of conformal antennas a full electromagnetic analysis is required. It is beyond the scope of this report to discuss this in detail, but some examples will be given where the electromagnetic properties are illustrated and the differences to conventionell planar antennas are emphasized.

When analysing array antennas (planar and conformal) the mutual coupling among the elements is the most important parameter to fully characterize the antenna. But, due to the curved surface, the mutual coupling behaves differently than for the planar case. This will also affect the characteristics of the antenna. One important parameter to discuss is the maximum gain that can be obtained with the proposed conformal array, as well as side lobe levels and polarization properties of the achieved radiation pattern. This will be illustrated next by some examples.

The first one is a hardware demonstrator developed at Ericsson Microwave Systems AB. The array in Figure 2.4-A consists of 18x3 rectangular waveguide apertures and is mounted at a metal cylinder with radius 30 cm [4].

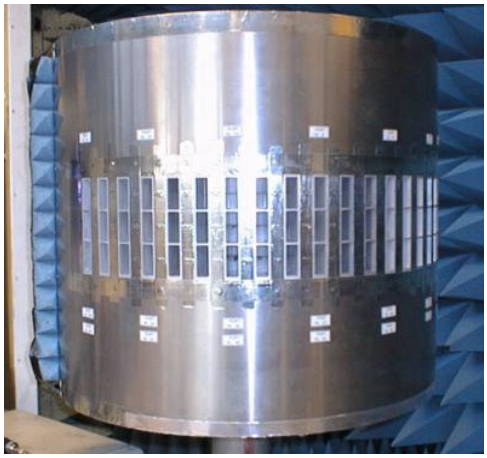

Figure 2.4-A: Cylindrical waveguide array demonstrator developed by Ericsson Microwave Systems AB

Figure 2.4-B. shows the mutual coupling along the circumferential direction of the circular cylinder. It is the E plane coupling compared with the planar case. Both isolated and array mutual coupling is considered, and rectangular waveguide-fed apertures are used as elements. Isolated coupling refers to the mutual coupling between two elements only, while the other elements of the array are assumed to be absent (short circuited in case of apertures). With all elements present, the term array mutual coupling is used. The amplitude of the coupling in the planar case decays as 1/*s*, where *s* is the element spacing. Obviously the surface field along the circumferential direction of the cylinder experiences a faster decay due to continuous leaking, resulting in an exponential decay due to the curvature. Furthermore, the effect of the elements in between is clearly visible in both amplitude and phase, although the phase is more sensitive to the presence of other elements than the amplitude (in both cases).

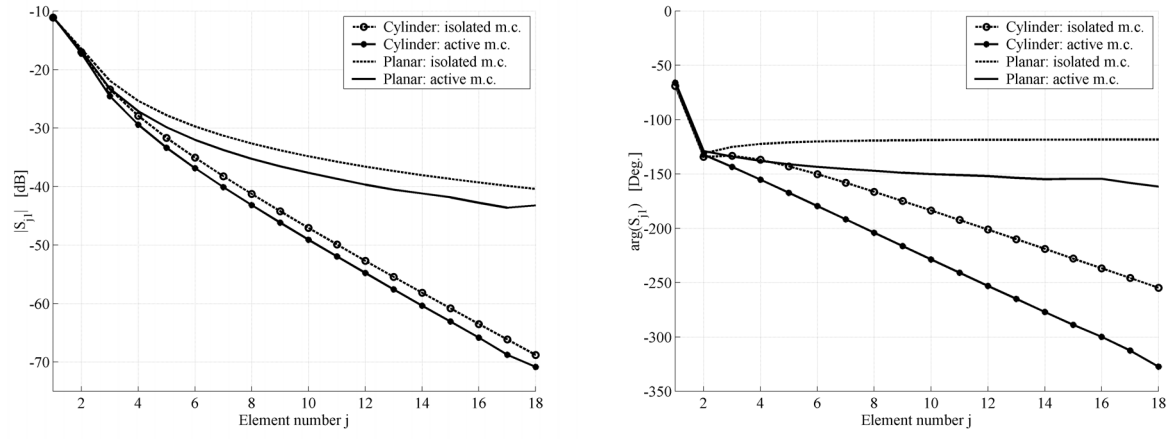

(a) (b)

Figure 2.4-B: A comparison between the array and isolated mutual coupling for a single row array on a cylinder (E plane). The corresponding planar case is also shown for a single row of 18 elements [4]. (a) magnitude, (b) phase

Figure 2.4-C shows the gain of the E plane embedded element pattern for a single ring of circumferentially polarized rectangular apertures for different cylinder radii. The element spacing is kept constant, equal to s=0.6λ. The patterns are also compared with those of the corresponding planar case. As seen, there are no major differences between the pattern for the planar case and the pattern for a cylinder with a large radius in the lit region. Both patterns exhibit a clearly visible drop-off near $\phi = 42°$. This drop-off in the planar case is due to an end fire grating lobe at $\phi = 41.8°$. Its counterpart in the cylindrical array is a “cylindrical end fire grating lobe” [12]. It should

be noted that the cylindrical grating lobe is not as distinct as in the planar case due to the curved surface. However, the phenomenon is caused by the same mechanisms in both cases.

Since the cylindrical grating lobe is more diffuse in the cylindrical case the pattern dips are not as deep as in the (infinite) planar case. We have in the cylinder case a finite number of elements participating, fewer the smaller the radius of the cylinder. The mutual coupling amplitude is also less for the curved case.

Another interesting observation is the ripple in the broadside (lit) region for the circular cylinder, not observed in the (infinite) planar case. This ripple is caused by the finiteness of the curved array, and is also observed in finite planar arrays [13] but not as pronounced as in the cylinder case.

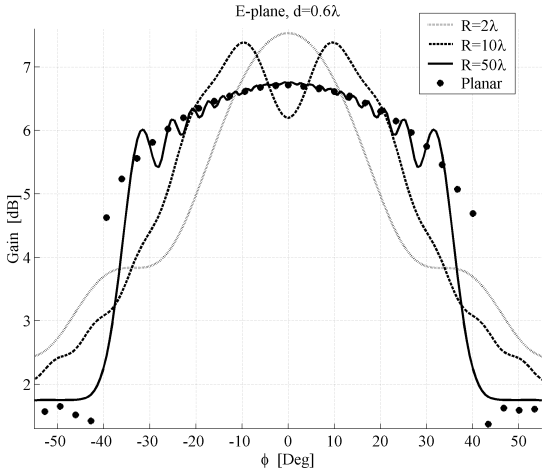

Figure 2.4-C: The gain of the E plane embedded element pattern for a single ring array in azimuth versus the radius of the cylinder for a fixed element spacing d=0.6λ [4]. Overview for R=2λ, 10λ, and 50λ, the corresponding planar case is also shown.

For planar and linear arrays analytical solutions are known to determine the weighting of the array elements, e.g. to achieve the maximum gain for a predefined side-lobe level. In the case of conformal arrays, where no common element factor exists, usually an element-by-element approach has to be used to determine the array pattern and only few analytical solutions for the optimum weighting, with respect to a desired radiation pattern, are known to date. Addressing the optimum array gain, A. Hessel and J.-C. Sureau have stated the following theorem [14]: The maximum realized gain of an array in a specified direction is equal to the sum of the individual element gain function values in the direction of interest. The appropriate excitation is such that the amplitudes are proportional to the respective element patterns in the direction of interest and the phases yield total phase correction for each element. The consequence of this theorem is that the antenna elements of the conformal array that point in directions that are very different from the direction of the main beam practically cannot be used since their optimum excitations are very low. Therefore, from practical reasons, an area of active elements is defined for each considered direction of the main beam.

This property of conformal antennas can be additionally illustrated in the following example [15]. In Figure 2.4-D the maximum directivity of a cylindrical array is considered as a function of the cylinder radius. The curves for the two reference cases ‘asymptote’ and ‘projected’ are plotted into the same figure; the reference cases correspond to the directivity obtained from the total area and from the projected area of the cylindrical array. We see that the directivity of cylindrical array always is lower than the directivity of planar array with the same projected aperture, but the difference is not very large. However, the angular scan range is much larger compared to a corresponding planar array. When the radius of the cylinder increases, the directivity asymptotically approaches the directivity of the projected planar array.

In planar or linear arrays polarization is typically determined by the single array element. Therefore, polarization is not an important issue for those array configurations. For conformal arrays things

change. The polarization properties of a cylindrical array are illustrated in Figure 2.4-E for the case when the beam is scaned in both ayimuthal and elevation directions to ϕ=30° and θ=30° [16]. It can be seen that the polarization can significantly vary over the radiation pattern. The polarization control is therefore one of the important issues when designing conformal arrays.

Since antenna elements of the conformal array point in different directions, conformal arrays in principal have larger side lobes comparing to the equivalent planar ones. For the same reason grating lobes of arrays with larger spacing between antenna elements have smaller amplitudes than the planar ones (Figure 2.4-F) [12].

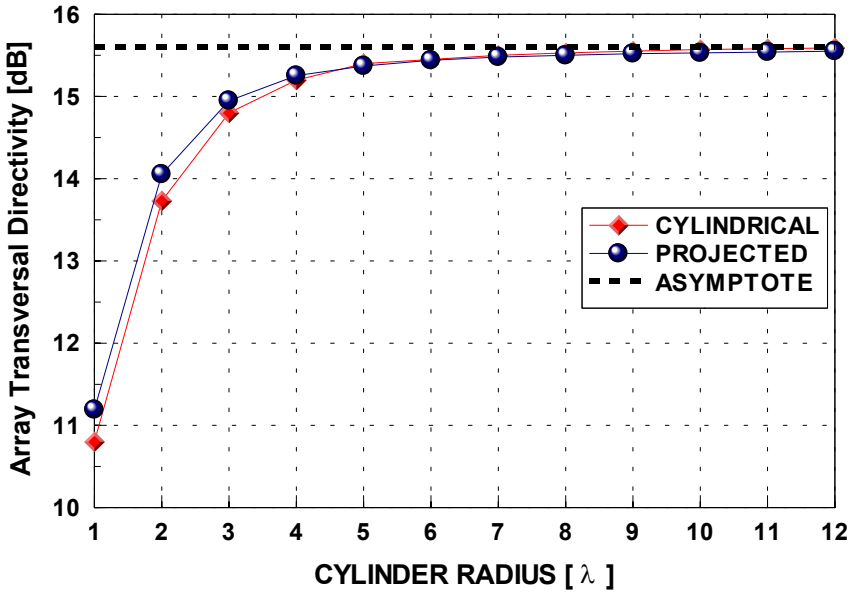

Figure 2.4-D: The transverse directivity of the optimized cylindrical arrays compared to the maximum available transverse directivity of the same array when the radius of curvature of the cylinder is infinite ('asymptote'), and of a planar array with the same projected aperture ('projected') [15].

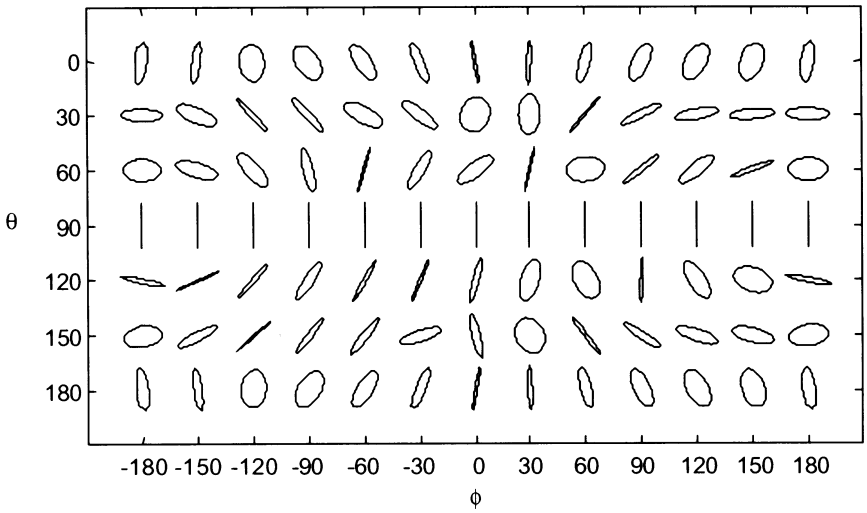

Figure 2.4-E: Polarization properties of the radiation pattern of cylindrical waveguide array [16].

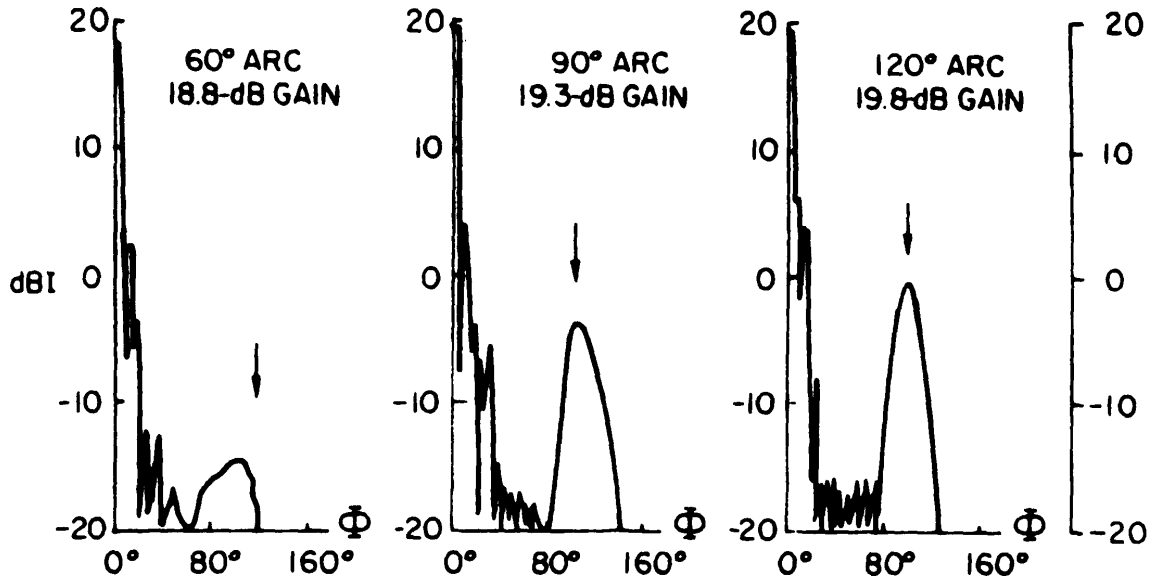

Figure 2.4-F: Dependence of gain and side lobe levels for different size of active sector of cylindrical array, taken from [12]: Radiation characteristics of sector arrays. Maximum gain E-plane patterns for sector arrays, occupying sectors of 60°, 90° and 120°.

2.5 History and near term goals

The start of conformal arrays can be traced at least back to the 1930s when a system of dipole elements arranged on a circle, thus forming a circular array, was analyzed by [11]. During the Second World War HF circular arrays were developed for radio signal intelligence gathering and direction finding in Germany. These so-called Wullenweber arrays were quite large with a diameter of about 100 meters. After the war an experimental Wullenweber[1] array was developed at the University of Illinois, see Figure 2.5-A. This array had 120 radiating elements in front of a reflecting screen. The diameter is about 300 meters, note the size of the buildings in the center [17].

Nose-mounted antennas in missiles or aircraft are protected by a pointed radome. Alternatively, the antenna elements could be put on the radome itself. This possibility has created an interest in conformal arrays on cones [18]. The progress in this field has been slow, however. Also conformal spherical antennas have attracted interest. A well-known example is the Dome Radar Antenna [19], [20], see Figure 2.5-B.

[1] J. Wullenweber, 1488-1537, Lord Mayor of Lübeck

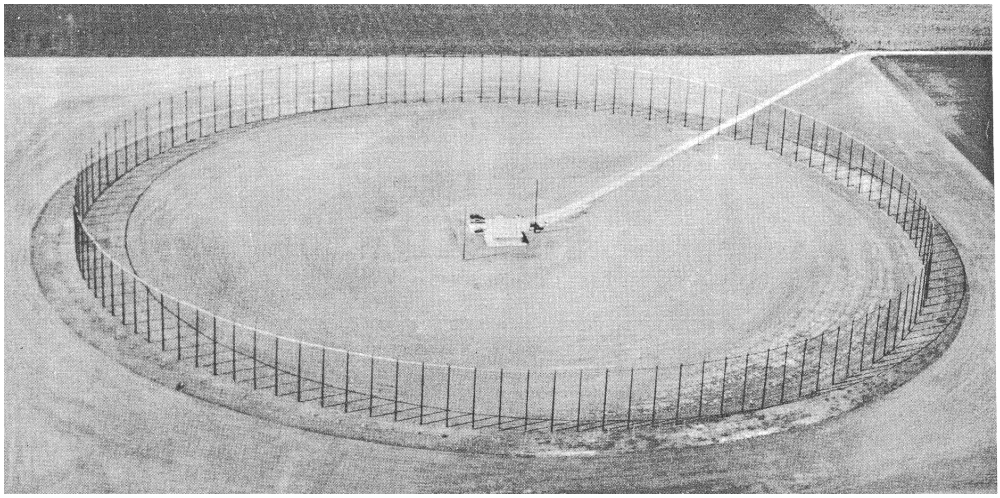

Figure 2.5-A: The experimental 300 m diameter Wullenweber antenna at the University of Illinois [17].

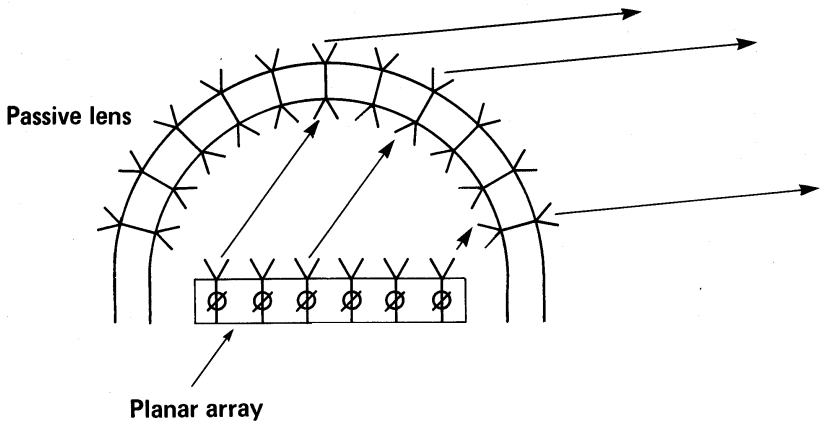

Figure 2.5-B: The Dome array concept using a single planar array and a passive lens for hemispherical coverage.

A paper in the Space/Aeronautics magazine in 1967 [21] presented a very optimistic view of the development of conformal arrays for nose radar systems in aircraft; see Figure 2.5-C. Obviously the development was not so quick. However, the conformal nose-mounted array has many advantages, especially an increased field of view compared to the traditional ±60° coverage with planar antennas.

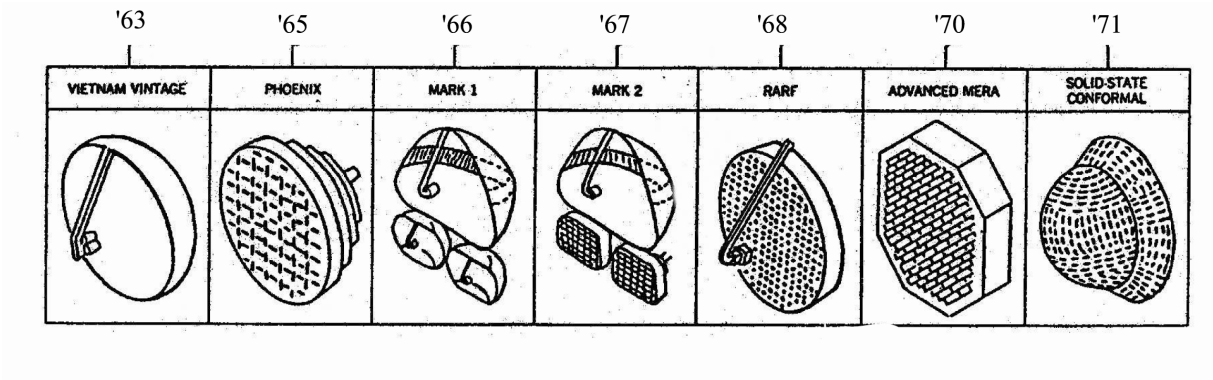

Figure 2.5-C: Predicted nose radar development as of 1967 [21].

A multibeam scanning antenna for an observation mission at an altitude around 800 km is presented in [22], [23]. The array was designed to give a high data rate while keeping low transmitted power and to enable simultaneous links with several ground stations. The conical array antenna for data communication, shown in Figure 2.5-D, consists of 24 subarrays with 6 elementary radiators on each. The array shape has been optimised to be compliant with a specified EIRP mask in the elevation plane.The mask determines a maximum power to be radiated at a scan angle of 62.3°, while the power in 0° direction may be reduced by 12dB.

Figure 2.5-D: A conical conformal array antenna [22], [23].

In [24], [25] two conformal phased array antenna concepts for INMARSAT terminals are presented. The desired angular coverage is 360° in azimuth and from –10° to 90° in elevation. The first approach for the antenna structure was a nearly spherical shaped array, consisting of 54 triangles, each containing 18 single antenna elements. Since this concept would have required too many TR-modules, it was dropped for cost reasons. The finally chosen approach, shown in Figure 2.5-E, will allow an electronically steerable beam in elevation direction from –10° to 100°, whereas the azimuth direction is steered mechanically. It is constructed from 64 subarrays, each containing four aperture coupled single radiating elements, placed on a cylindrical surface, which merges into a flat array. To avoid fast mechanical turns when tracing in the zenith region, the scanning range in elevation is exceeded to 10° beyond zenith.

Another array for satellite communication from mobiles, is shown in Figure 2.5-F. The antenna is made up of 40 identical triangular tiles, each containing six cross-dipole elements. The antenna array structure is based upon a modified dodecahedron and in the size of a small football. Each tile contains all the electronics and signal combining to form a multi-layer microwave circuit board. GaAs MMICs provide the necessary LNA, phase shifting and PA functions to achieve a full duplex array covering 7.25 to 8.4 GHz. The electronically steered beam covers the full upper hemisphere as well as down to -10 degrees elevation [26].

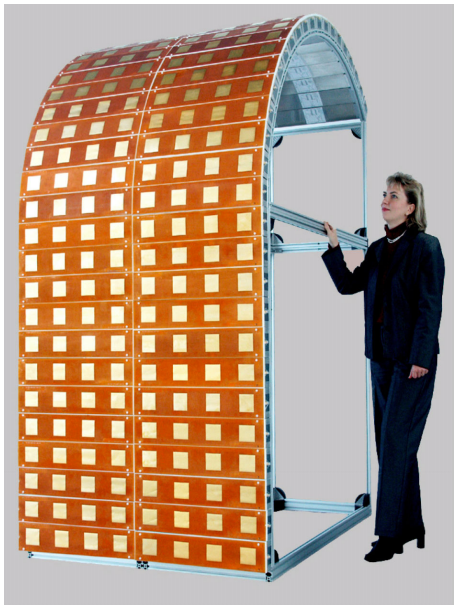

Figure 2.5-E: Patch array for an active low cost steerable antenna for multimedia satellite communication [25].

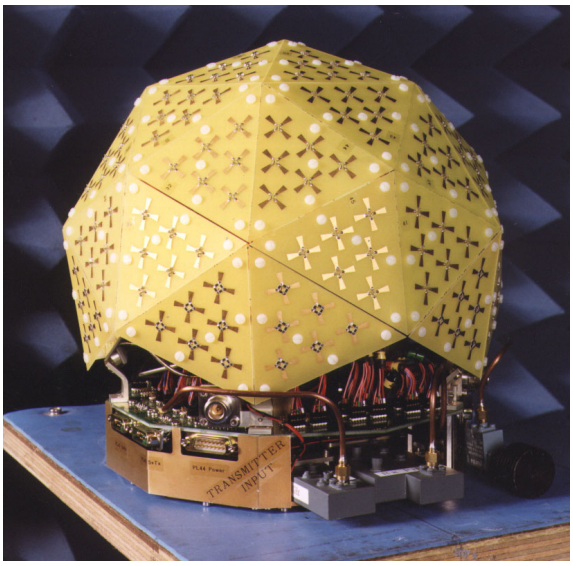

Figure 2.5-F: A faceted active array antenna with six dual polarized dipole elements in each facet [26].

In [27], a spherical array antenna applicable to mobile satellite communication is presented. The fabricated hemispherical antenna shown in Figure 2.5-G has a diameter of 344 mm and consists of 16 circular patches operating at 1.54 GHz with circular polarization. The measured antenna gain varies slightly from 14.7 dBi at zenith to 13.6 dBi at 30° elevation and 11.6 dBi at 0° elevation. The antenna substrate is made of modified Polyphenylene Oxide resin and is vacuum formed over a wooden mold. This technique may also be applied to any other curved surface.

A flexible and light-weight antenna composed of a flexible woven conductive fabric and a felt is presented in [28] and shown in Figure 2.5-H. It can be easily sewn into clothing and may be applied as a GPS antenna, or an array of elements may form the terminal antenna for personal satellite communications.

Figure 2.5-G: An experimental L-band conformal array antenna for mobile satellite communication systems [27].

Figure 2.5-H: A wearable antenna for GPS receiving [28].

Future mobile base stations can be concealed for aesthetical reasons, see Figure 2.5-I.

Figure 2.5-I: Possible future locations for base station antennas [29].

The most important application of the conformal antenna concept in the long term future will be found in the smart skin approach, which envisages the integration of non-planar active antenna apertures in curved surfaces adapted to the skin of the platform (aircraft, satellite, car etc.), see next Section 2.6.

2.6 Long term goals

A vision of a future smart skin conformal antenna is shown in Figure 2.6-A. This antenna constitutes a complete RF system, including not only the radiating elements but also feed networks, amplifiers, control electronics, power distribution, cooling, filters etc., all in a flexible design that can be tailored to various structural shapes [30], [31]. Note, the system may include other types on sensors as well, not only electromagnetic antennas. However, to reach this smart skin goal is quite demanding. The biggest problems are the analysis and construction of these antennas/sensors. For example, there are a number of different sensors that should work together without disturbing the function of each other. Furthermore, the mechanical construction should be adjustable to different surfaces and at the same time strong enough for any possible strain that could be the case on e.g. an aircraft or satellite [32]-[34].

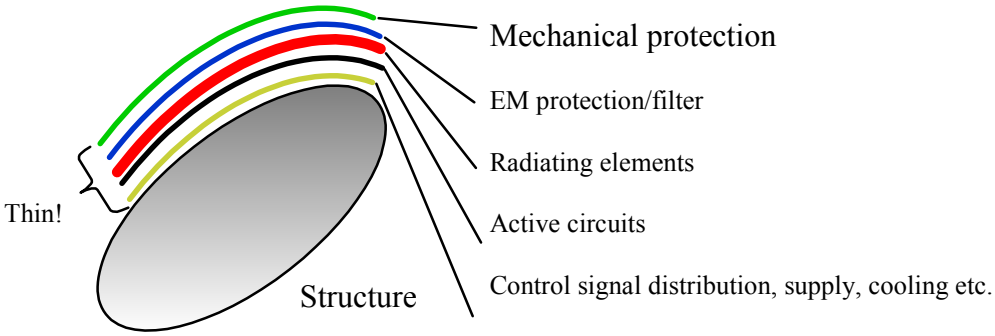

Figure 2.6-A: The smart skin vision [30].

2.7 References

[1] S. W. Schneider, C. Bozada, R. Dettmer, and J. Tenbarge: Enabling Technologies for Future Structurally Integrated Conformal Apertures. IEEE AP-S Int. Symp. Digest, Boston, pp. 330-333, 8-13 July 2001.

[2] D. A. Wingert and B. M. Howard: Potential Impact of Smart Electromagnetic Antennas on Aircraft Performance and Design. NATO Workshop on Smart Electromagnetic Antenna Structures, Brussels, pp. 1.1–1.10, November 1996.

[3] M. A. Hopkins, J. M. Tuss, A. J. Lockyer, K. Alt, R. Kinslow, and J. N. Kudva, Smart Skin Conformal Load-bearing Antenna and Other Smart Structures Developments, American Inst. Aeronaut. Astronaut. (AIAA), Structures, Structural Dynamics & Materials Conf., Vol. 1, pp. 521-530, 1997.

[4] L. Josefsson and P. Persson, Conformal Array Antenna Theory and Design, Wiley-IEEE Press, January 2006, in print (http://www.wiley.com/WileyCDA/WileyTitle/productCd-0471465844.html).

[5] N. Amitay, V. Galindo, and C. P. Wu: Theory and analysis of phased array antennas, New York, Wiley-Interscience, 1972.

[6] R. F. E. Guy: Method of Obtaining a Regular Element or Beam Conformal Array Lattice applied to a Luneberg Lens with a Concave Spherical Array Feed. Proc. of the 4th European Workshop on Conformal Antennas, Stockholm, Sweden, 2005.

[7] C. D. Watkins: WEAO Collaborative Research on Conformal Antennas and Military Radar Applications. Proc. of the 2nd European Workshop on Conformal Antennas, The Hague, The Netherlands, 2001.

[8] L. Josefsson and M. Lanne: Shape Optimization of Doubly Curved Conformal Array Antennas. Proc. of the 3rd European Workshop on Conformal Antennas, Bonn, Germany, 2003, pp. 137-139.

[9] G.H. Knittel: Choosing the number of faces of a phased array antenna for hemisphere scan coverage. IEEE Trans. Antennas Propagat., Vol. 13, November 1965, pp. 878-882.

[10] T. K. Wu: Phased array antenna for tracking and communication with LEO satellites. IEEE Int. Symp. on Phased Array Systems and Technology, 15-18 Oct 1996, pp 293-296.

[11] H. Chireix: Antennes à Rayonnement Zénithal Réduit. L'Onde Electrique, Vol. 15, pp. 440-456, 1936.

[12] R. Mailloux: Phased Array Antenna Handbook, Artech House, 1994.

[13] N. Amitay, V. Galindo, and C. P. Wu: Theory and analysis of phased array antennas, New York, Wiley-Interscience, 1972.

[14] A. Hessel and J. C. Sureau: On the Realized Gain of Arrays. IEEE Trans. on Antennas and Propagation, Vol. AP-19, No. 1, January 1971, pp.122-124.

[15] N. Herscovici, Z. Sipus, P.-S. Kildal, S. Raffaelli: Excitations maximizing the directivity of conformal array on circular cylinders. 2nd European Workshop on Conformal Antennas, The Hague, The Netherlands, April 2001.

[16] N. Calander and L. Josefsson: A look at polarization properties of cylindrical array antennas. 2nd European Workshop on Conformal Antennas, The Hague, The Netherlands, April 2001.

[17] P. J. D. Gething: High-Frequency Direction Finding, Proc. IEE, Vol. 113, No. 1, pp. 49-61, January 1966.

[18] A. D. Munger, G. Vaughn, J. H. Provencher, and B. R. Gladman: Conical Array Studies. IEEE Trans. Antennas Propagation, Vol. AP-22, No. 1, pp. 35-43, January 1974.

[19] S. V. Bearse: Planar Array Looks Through Lens to Provide Hemispherical Coverage. Microwaves, July 1975, pp.9-10.

[20] P. M. Liebman, L. Schwartzman, and A. E. Hylas: Dome Radar - A New Phased Array System. IEEE Int. Radar Conf., Washington, D. C., pp. 349-353, 1975.

[21] P. G. Thomas: Multifunction Airborne Radar. Space/Aeronautics, February 1967, pp. 74-85.

[22] E. Vourch, G. Caille, M. J. Martin, J. R. Mosig, A. Martin, and P. O. Iversen: Conformal Array Antenna for LEO Observation Platforms, IEEE AP-S Int. Symp. Digest, pp. 20-23, 1998.

[23] G. Caille, E. Vourch, M. J. Martin, J. R. Mosig, and A. Martin Polegre: Conformal Array Antenna for Observation Platforms in Low Earth Orbit, IEEE Antennas Propagat. Magazine, Vol. 44, No. 3, pp. 103-104, June 2002.

[24] D. Löffler, W. Wiesbeck, M. Eube, K.-B. Schad, and E. Ohnmacht: Low Cost Conformal Phased Array Antenna Using High Integrated SiGe-Technology. Proc. of the IEEE Antennas and Propagation Society International Symposium, Boston, Mass, USA, July 8-13, 2001, vol. 2, pp. 334-337.

[25] F. Pivit, D. Löffler, W. Wiesbeck,M. Bötcher, and M. Eube: Patch Array Design for an Active Low Cost Steerable Antenna for Multimedia Satellite Communication(ALCANT). Proc. of the 3rd European Workshop on Conformal Antennas, Bonn, Germany, 2003, pp. 87-90.

[26] Website: http://www.roke.co.uk/sensors/antennas/agile_phased_array.asp, 2005-09-17.

[27] W. Chujo, Y. Konishi, Y. Ohtaki, and K. Yasukawa: Performances of a Spherical Array Antenna Fabricated by Vacuum Forming Technique, Proc. 20th European Microwave Conf., pp. 1511 - 1516, Sept. 1990.

[28] M. Tanaka and J. H. Jang: Wearable Microstrip Antenna. IEEE AP-S Int. Symp. 2003 Digest, vol. 2, pp. 704 - 707, 22-27 June 2003, Colubus, Ohio, USA.

[29] Website: http://www.stealthsite.com/index.htm, 2005-09-13.

[30] L. Josefsson: Smart Antennas for the Future. RVK 99, Karlskrona, Sweden, pp. 682-685, June 1999.

[31] P. Baratault, F. Gautier, and G. Albarel: Évolution des Antennes pour Radars Aéroportés. De la Parabole aus Peaux Actives. Rev. Techn., Thomson-CSF, pp. 749-793, September 1993.

[32] M. Caplot, J.-M. Chabroux, T. Lemoine and J.-P. Martinaud: Conformal Antenna Integration in Future Military Systems. Workshop on Smart Electromagnetic Antenna Structures, NATO Headquarters, Brussels, pp. 6.1-6.6, November 1996.

[33] A. F. Fray, L. D. Bamford, and A. Tennant: Aircraft Antenna Array Technology. Workshop on Smart Electromagnetic Antenna Structures, NATO Headquarters, Brussels, pp. 5.1-5.13, November 1996.

[34] V. K. Varadan and V. V. Varadan: Design and Development of Smart Skin Conformal Antenna. Workshop on Smart Electromagnetic Antenna Structures, NATO Headquarters, Brussels, pp. 12.1-12.16, November 1996.

2.8 List of Acronyms

EIRP	Equivalent Isotropic Radiated Power
GPS	Global Positioning System
KTH	Kungliga Tekniska Högskolan
LNA	Low Noise Amplifier
MMIC	Millimetre Wave Integrated Circuit
NoE	Network of Excellence
RCS	Radar Cross Section
TR	Transmit/Receive
TUD	Technische Universität Darmstadt
UAV	Unmanned Aerial Vehicles

3 BENCHMARKING STRUCTURES

3.1 Introduction

Nowadays, design of antennas relies mostly on accuracy and speed of used electromagnetic software. There are two criteria in selecting the appropriate software tool: to use general programs like FDTD or FEM, or to use specialized programs developed for specific geometry. The conformal antenna structures are usually large in terms of the wavelength, and consequently the needed computer time can be very large if a general program is selected for design procedure. It is more convenient to use specialized programs for specific conformal geometries that are fast and in some cases more accurate since they explicitly take into account the antenna geometry. Therefore, the usual procedure in designing conformal antennas is first to use a specialized program for a specific type of conformal antennas, and then to use some general program for designing fine details.

Before determining the antenna parameters, the designer should know what is the accuracy of the software proposed for the design process. The practice has shown that even the expensive commercial software packages can easily introduce a large error, i.e. the obtained design is useless in that case. Furthermore, working with commercial CAD tool requires costly training sessions and long-term experience. The best performances of commercial software tool can be obtained only by experienced engineers. In other words, it is not acceptable to waste a couple of weeks before it is discovered that the antenna structure is treated in a wrong way, or that the software tool cannot correctly handle the considered structure! Therefore, maybe the best way to test if one program is suitable for designing some particular antenna is to analyze some benchmarking structure that is similar to the considered antenna. In that way the engineers will see if the proposed software is accurate enough, and if the software is used in a proper way.

In summer 2005 all members of the work project WP 2.4-3 filled a questionnaire about suitable benchmarking structures for conformal antennas. As a result, nine structures are proposed for benchmarking activity. The structures cover cylindrical, spherical, conical and parabolic conformal geometries. As radiating elements, microstrip patch antennas and waveguide openings are proposed. Therefore, we believe that we have covered a large group of conformal antennas, i.e. most of the developed conformal antennas have similarity with at least one of the proposed structures. The list of the proposed structures is given in the next table, and their pictures are given in Figures 3.1-A to 3.1-D.

The goal of the benchmarking activity is twofold. First, we would like to fully describe the proposed benchmarking structures in order to enable antenna engineers simply to check the considered programs. In other words, all the parameters of the considered antenna should be given, as well as the measured data (from practical reasons, the measured data should be given in the form of ASCII files). Second, we would like to explore what is the accuracy of the developed software for analyzing conformal antennas. By this, possible users will see if the developed software fulfils their needs (accuracy, speed).

To summarize, the main achievements within this work-package during the last 9 months are the following:

- Collection of conformal benchmarking structures among ACE WP 2.4-3 participants
- Selection of 3 typical benchmarking structures and organization of preliminary testing of conformal antenna software.

The benchmarking process will be finished in ACE-2, and we will follow the procedure established in the WP 1.1-2 that is dedicated to the assessment of antenna software. In this report we will give preliminary results for three geometries: cylindrical waveguide array, cylindrical sector patch antenna, and spherical patch array.

Structure description	Institution	Type of geometry	Type of radiating elements	Type of feeding structure
Cylindrical waveguide array	EMW	Circular-cylindrical	Rectangular waveguides	Rectangular waveguide
Parabolic waveguide array	EMW	Parabolic	Circular waveguides	Circular waveguide
φ-polarized cylindrical sector microstrip antenna	DLR	Circular-cylindrical	Rectangular patch	Microstrip transmission line
Axially-polarized cylindrical sector microstrip antenna	DLR	Circular-cylindrical	Rectangular patch with a notch	Microstrip transmission line
Axially-polarized circular cylindrical microstrip antenna	DLR	Circular-cylindrical	Rectangular patch with a notch	Microstrip transmission line
Quasi-cylindrical (conical) microstrip antenna	DLR	Conical	Rectangular patch with a notch	Microstrip transmission line
Spherical microstrip array	Chalmers	Spherical	Rectangular patch	Coaxial transmission line
Cylindrical waveguide array	TNO	Circular-cylindrical	Rectangular waveguides	Rectangular waveguide
Faceted waveguide array	TNO	Faceted	Rectangular waveguides	Rectangular waveguide

Table 3.1-A. Summary of the proposed benchmarking structures.

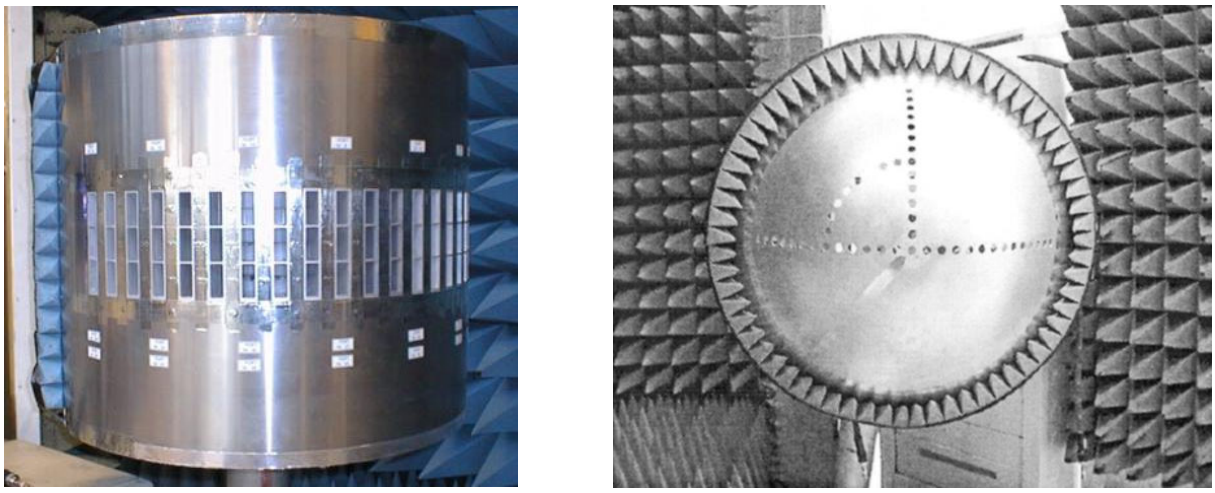

Figure 3.1-A. Waveguide demonstrators designed and constructed by EMW.
(a) cylindrical demonstrator, (b) parabolic demonstrator.

Figure 3.1-B. Cylindrical sector patch antenna and conical patch antenna built at DLR.

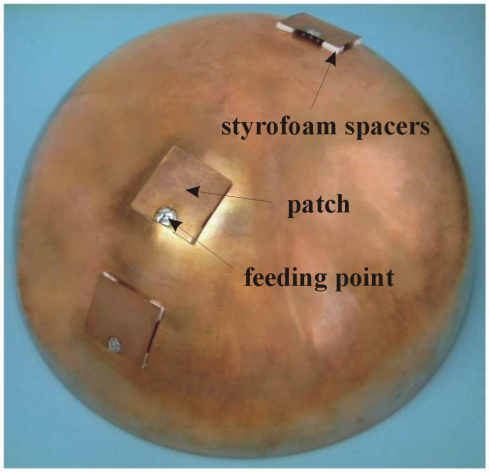

Figure 3.1-C. Spherical patch array (CHALMERS and University of Zagreb)

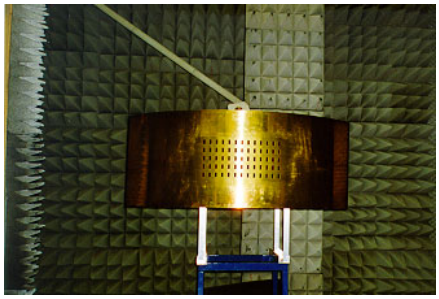

a)

b)

Figure 3.1-D. Cylindrical array of X-band open-ended rectangular waveguides, a) without radome, b) with radome

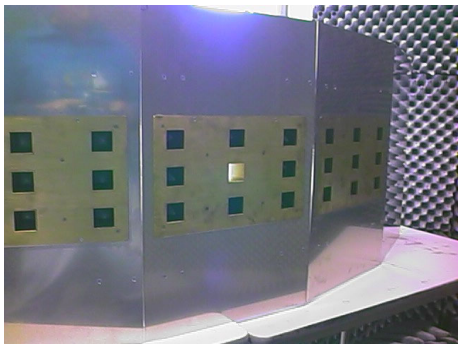

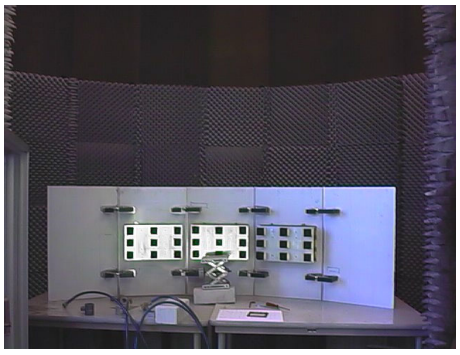

Figure 3.1-E. Faceted array of X-band open-ended rectangular waveguides

In [1] we have given the description of developed programs for analyzing conformal antennas. All the considered software packages are for a specific type of conformal antennas and for specific antenna elements (waveguide openings, patches or dipoles). All of the programs use the moment method as a numerical method for determining the unknown physical or equivalent currents (the exception is the CylFDTD program which is based on FDTD in cylindrical coordinate system). The main difference is in the type of structures they can analyse, and how the expressions needed for the moment method procedure are numerically calculated. The developed programs are listed in next table.

Name of the program	***Developer***	***Type of structure***	***Type of radiating elements***
Cylindrical Magmas	K.U. Leuven	• Multilayer circular-cylindrical structures	• Patches
DMM	DLR	• Structures consisting of quasi-planar multilayer parts	• Patches
MCAT	DLR	• Multilayer circular-cylindrical structures	• Patches
G1DMULT	Chalmers	• Multilayer circular-cylindrical structures • Multilayer spherical structures	• Patches • Waveguide apertures
G2DMULT	Chalmers	• Multilayer cylindrical structures with arbitrary cross-section	• Patches • Dipoles • Waveguide apertures
CylFDTD	FOI	• Multilayer circular-cylindrical structures	• Waveguide apertures
Conformal Antenna Design	KTH	• Single-curved PEC surfaces • Doubly-curved PEC surfaces • Coated PEC circular-cylinders	• Waveguide apertures
MEN_MFSS	TNO	• Multilayer circular-cylindrical structures including FSS	• Waveguide apertures

Table 3.1-B. Summary of the developed software for analyzing conformal structures.

References

[1] ACE WP 2.4-3, Deliverable 2.4-D6: “Conformal Antennas: Inventory of the on-going research.”

3.2 Structure 1: Circular-cylinder waveguide array

3.2.1 Structure description

1- Entity

Ericsson Microwave Systems AB, SE-431 84 Molndal, Sweden.
Maria Lanne, maria.lanne@ericsson.com, marialan@s2.chalmers.se, +46 31 747 05 22

2- Structure Definition

The radius of the circular cylinder is 0.30 m and each of the three rows of elements covers a 120° sector in ϕ-direction. The waveguide apertures have dimension 39 x 16 mm (z- x ϕ-direction) and are polarized in ϕ-direction. The element distance is dz x dϕ = 41 x 37.1 mm (H-plane x E-plane). The cylindrical metal surface continues 0.22 m outside the aperture.

Each waveguide element can either be connected to measurement equipment or terminated in matched loads.

A radome of dielectric material can be placed in front of the aperture. The cover has a thickness of 3.99 mm and ε_r=2.4. The array without the radome is shown in Figure 3.2-A.

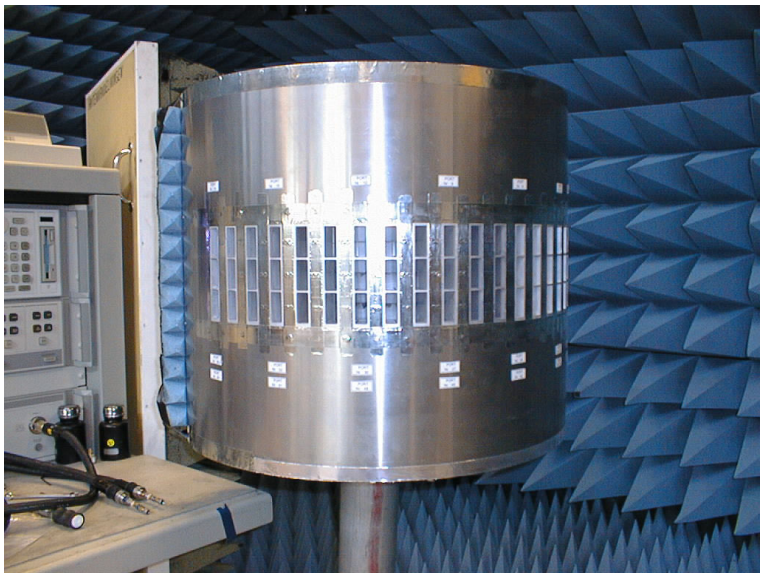

Figure 3.2-A. The cylindrical array without the radome.

3- Expected results

Measurements of mutual coupling in the E-plane are available for the frequencies 4.3 GHz and 5.65 GHz, both with and without the dielectric radome present. The mutual coupling was measured between two elements at a time. Both isolated (surrounding elements short-circuited using metal tape) mutual coupling and array (surrounding elements terminated in matched loads) mutual coupling have been measured from the first element in the upper row, to all the other elements in that row.

The element radiation patterns for one of the elements in the centre of the array are measured both in the E- and in the H-plane, both with and without the dielectric radome present. These measurements have been performed at the frequencies 4.9 GHz and 5.65 GHz. Both isolated (surrounding elements short circuited using metal tape) element patterns and active/embedded (surrounding elements terminated in matched loads) element patterns have been measured.

4- Interest of the structure

The circular cylindrical shape is a canonical shape, which is well suited for theoretical analysis. A circular cylindrical shape has also a wide range of applications.

5- Keywords

Circular cylindrical waveguide array, rectangular waveguide openings, dielectric radome, C-band, mutual coupling, element patterns

6- References

The measurement results have been compared with theoretical results, and papers have been written in cooperation with e.g. P. Persson at KTH, Z. Sipus at University of Zagreb, and B. Thors, currently at Ericsson AB. The references are listed below.

[1] L. Josefsson and P. Persson, “Conformal Array Synthesis Including Mutual Coupling”, *Electronic Letters*, Vol. 35, No. 8, pp. 625-627, 15th April 1999.

[2] P. Persson and L. Josefsson, “Calculating the Mutual Coupling Between Apertures on a Convex Circular Cylinder Using a Hybrid UTD-MoM Method”, *IEEE Trans. Antennas Propagat.*, Vol. 49 , No. 4, pp. 672-677, April 2001.

[3] Z. Sipus, S. Rupcic, M. Lanne, and L. Josefsson, “Moment Method Analysis of Circular-Cylindrical Array of Waveguide Elements Covered with a Radome”, *AP–S/URSI*, Boston, MA, USA, July 2001.

[4] Z. Sipus, S. Rupcic, M. Lanne, L. Josefsson, and P. Persson, “Analysis of Circular-Cylindrical Array of Waveguide Elements Using Moment Method”, *EMB01*, Uppsala, Sweden, Nov. 2001.

[5] P. Persson and R. G. Rojas, “High-frequency Approximation for Mutual Coupling Calculations Between Apertures on a Perfect Electric Conductor Circular Cylinder Covered with a Dielectric Layer: Nonparaxial Region”, *Radio Sci.*, Vol. 38, No. 4, 1079, doi:10.1029/2002RS002745, 2003.

[6] B. Thors and L. Josefsson, “Radiation and scattering trade-off design for conformal arrays”, *IEEE Trans. Antennas Propagat.,* Vol. 51, No. 5, pp. 1069-1076, May 2003.

[7] L. Josefsson and P. Persson, Conformal Array Antenna Theory and Design, IEEE Press, in print.

7- Applicability

See references above.

8- Confidentiality

There are no restrictions concerning the use of the proposed structure as an ACE benchmarking structure, but when results and/or pictures are shown of the array, reference should be made to Ericsson Microwave Systems AB, SE-431 84 Mölndal, Sweden.

3.2.2 Structure measurements

We have measured:

1. Mutual coupling in the E-plane for the frequencies 4.3 GHz and 5.65 GHz, both with and without the dielectric radome present. The coupling coefficients have been measured from the first element in the upper row, to all the other elements in that row. The isolated mutual coupling (surrounding elements short-circuited using metal tape) is given in Figs. 3.2-B and 3.2-C, and the array mutual coupling (surrounding elements terminated in matched loads) is given in Figs. 3.2-D and 3.2-E.

2. The element radiation patterns for one of the waveguide elements in the centre of the array. The working frequency has been 4.9 GHz and 5.65 GHz, and the element patterns have been measured both in the E- and in the H-plane, both with and without the dielectric radome present. The embedded (active) element patterns in the E-plane (surrounding elements terminated in matched loads) are given in Figs. 3.2-F and 3.2-G.

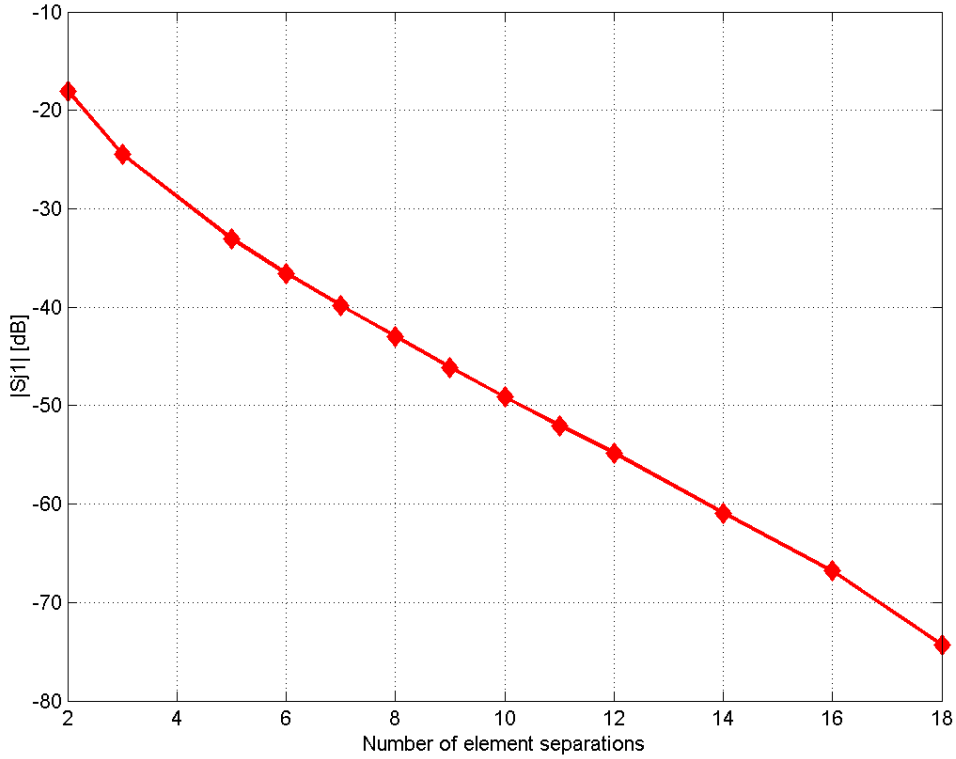

Figure 3.2-B. Isolated mutual coupling at frequency 5.65 GHz. No radome is present.

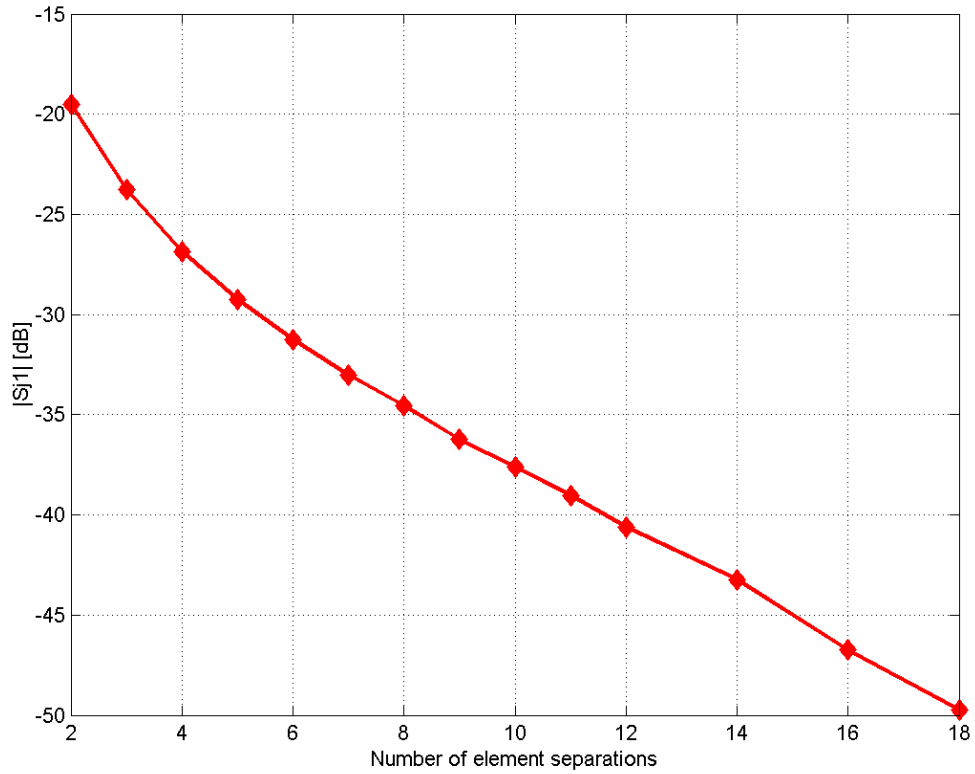

Figure 3.2-C. Isolated mutual coupling at frequency 5.65 GHz. Radome is present.

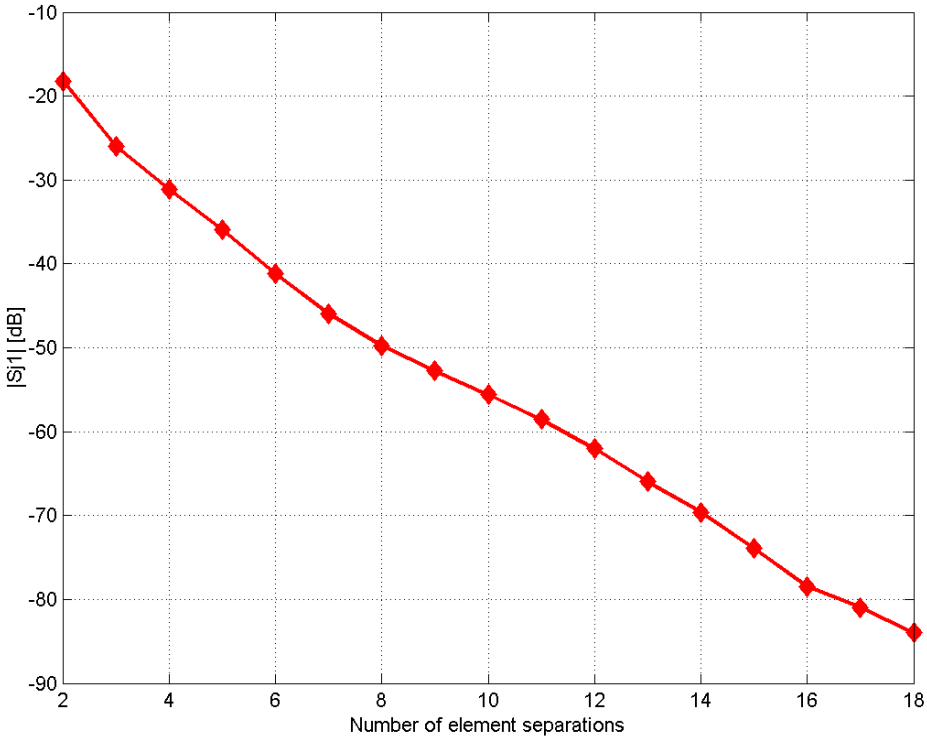

Figure 3.2-D. Array mutual coupling at frequency 5.65 GHz. No radome is present.

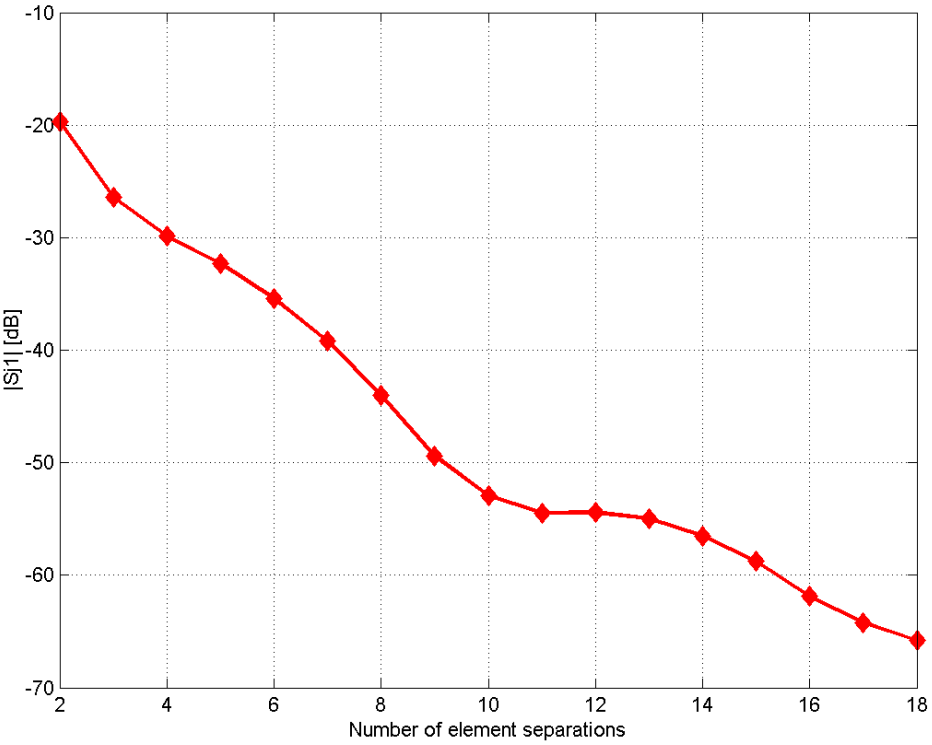

Figure 3.2-E. Array mutual coupling at frequency 5.65 GHz. Radome is present.

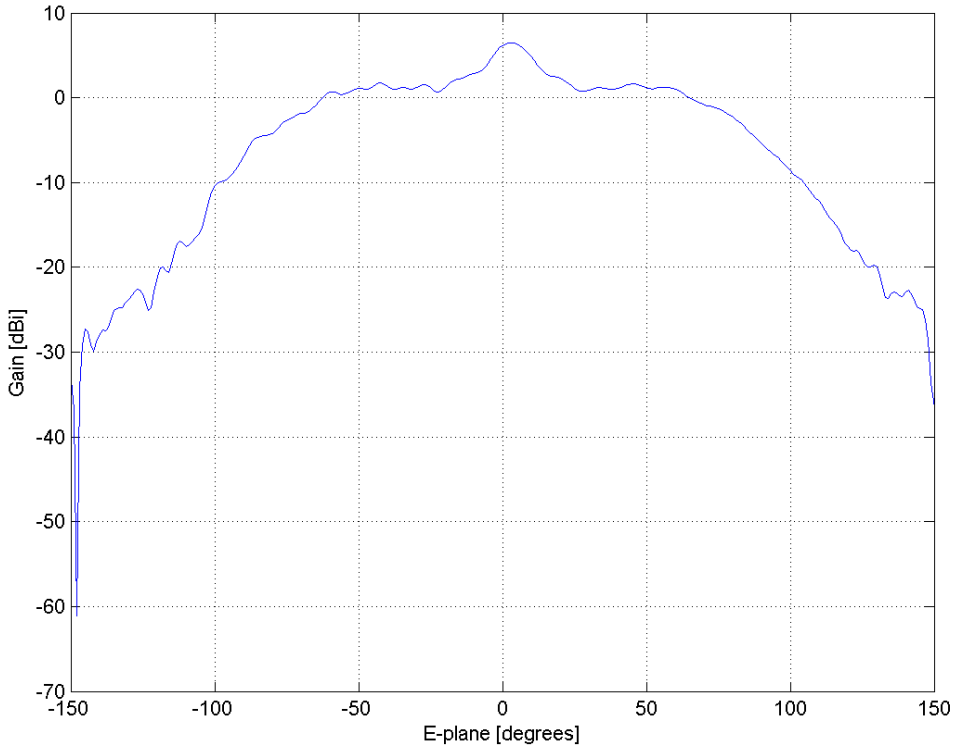

Figure 3.2-F. Embedded (active) element pattern in E-plane at frequency 5.65 GHz. No radome is present.

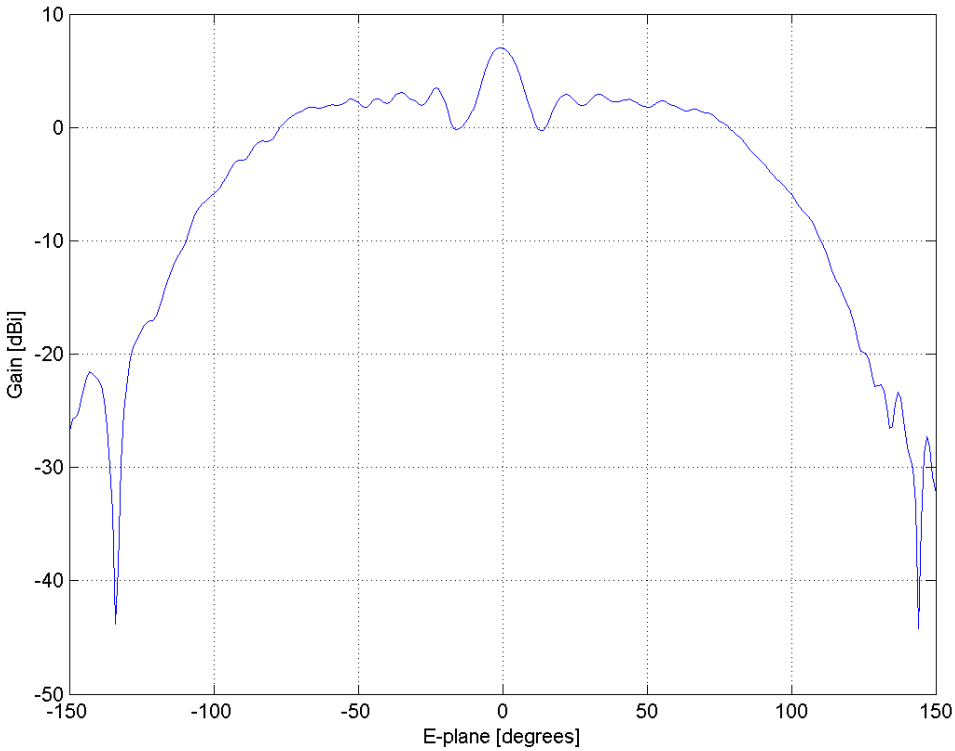

Figure 3.2-G. Embedded (active) element pattern in E-plane at frequency 5.65 GHz. Radome is present.

3.2.3 Simulated results by CHALMERS and University of Zagreb

1- Entity

Contact person: Zvonimir Sipus
Chalmers University of Technology
Department of Signals and Systems
SE-412 96 Gothenburg
Sweden
e-mail: zvonimir@s2.chalmers.se, zvonimir.sipus@fer.hr

2- Name of the simulation tool

G1DMULT - Program for analyzing conformal microstrip and waveguide arrays

3- Generalities about the simulation tool

G1DMULT is an IE-MoM based solver for modeling waveguide arrays and microstrip patch arrays embedded in circular-cylindrical or spherical multilayer structures. It is assumed that the waveguides or patches have rectangular shape, and three types of feeding structure are considered for microstrip patch antennas: microstrip transmission line, coaxial transmission line and aperture coupling.

4- Simulation Set-up (Geometry set-up, GUI, mesh, boundary conditions, excitation)

The geometrical structure was described in an input text file. Since the structure posses circular-cylindrical symmetry and since the radiating structure (waveguide opening) has a simple rectangular shape, the antenna can be described with a few parameters.

There is no need for meshing since the program uses the entire-domain basis functions.

The software assumes that the dielectric layers and grounded planes completely follow the cylindrical or spherical symmetry (e.g. the cylindrical structure is infinite in the axial direction). The radiating boundary conditions are implicitly implemented into the Green's functions; the metal parts are modeled by PEC boundary conditions. It is assumed that only the dominant mode can propagate inside the waveguides, i.e. all other modes are evanescent. Note that the evanescent modes are considered at discontinuity position, i.e. at the waveguide openings. No additional geometry is required by a simulator. The program almost immediately inputs the geometry and sets up the rest of simulations.

5- Simulation results

The results that have been computed are:

1. Input admittance at input port
2. Mutual coupling between two antenna elements (Figures 3.2-H to 3.2-K)
3. Embedded (active) element pattern, i.e. radiation pattern of an antenna element in the array environment (Figures 3.2-L and 3.2-M).

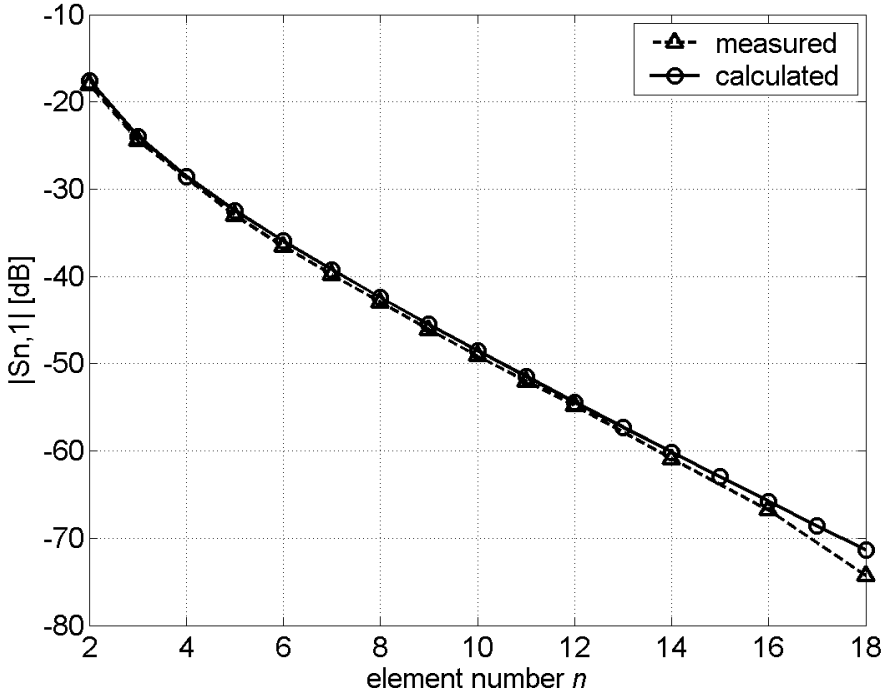

Figure 3.2-H. Isolated mutual coupling at frequency 5.65 GHz. Radome is not present.

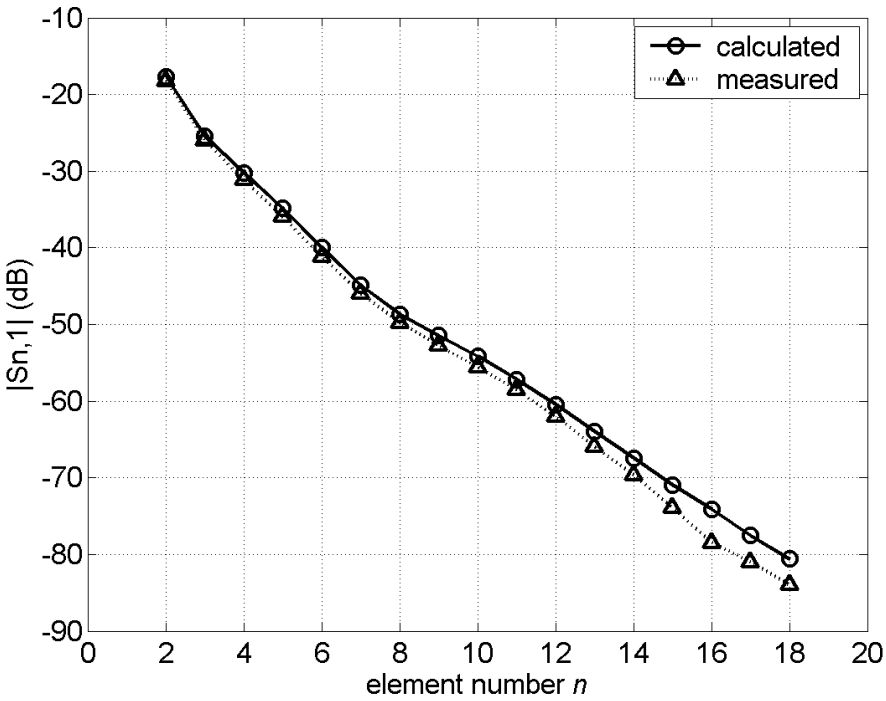

Figure 3.2-I. Array mutual coupling at frequency 5.65 GHz. Radome is not present.

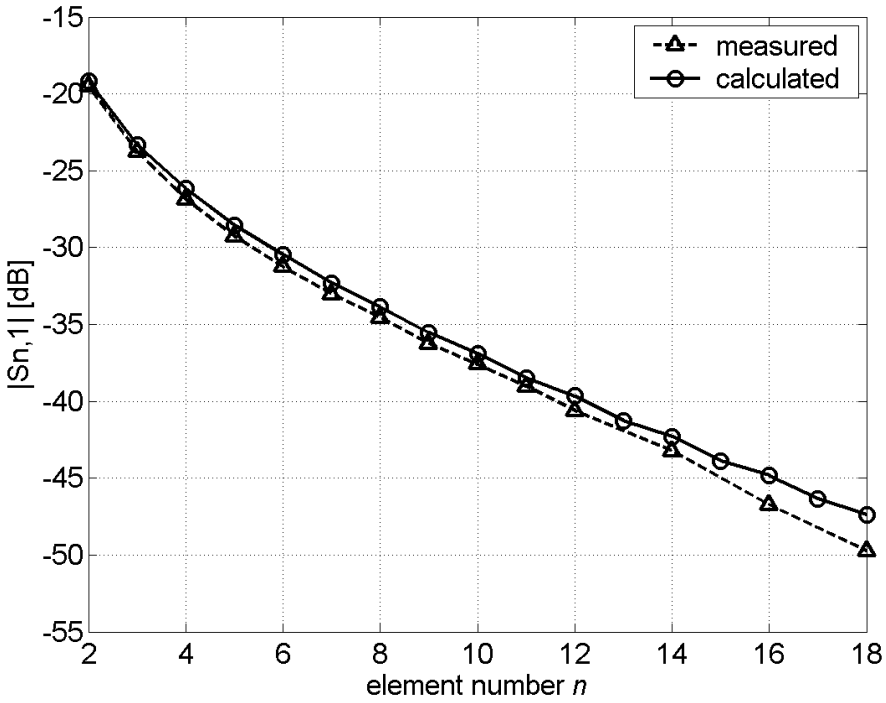

Figure 3.2-J. Isolated mutual coupling at frequency 5.65 GHz. Radome is present.

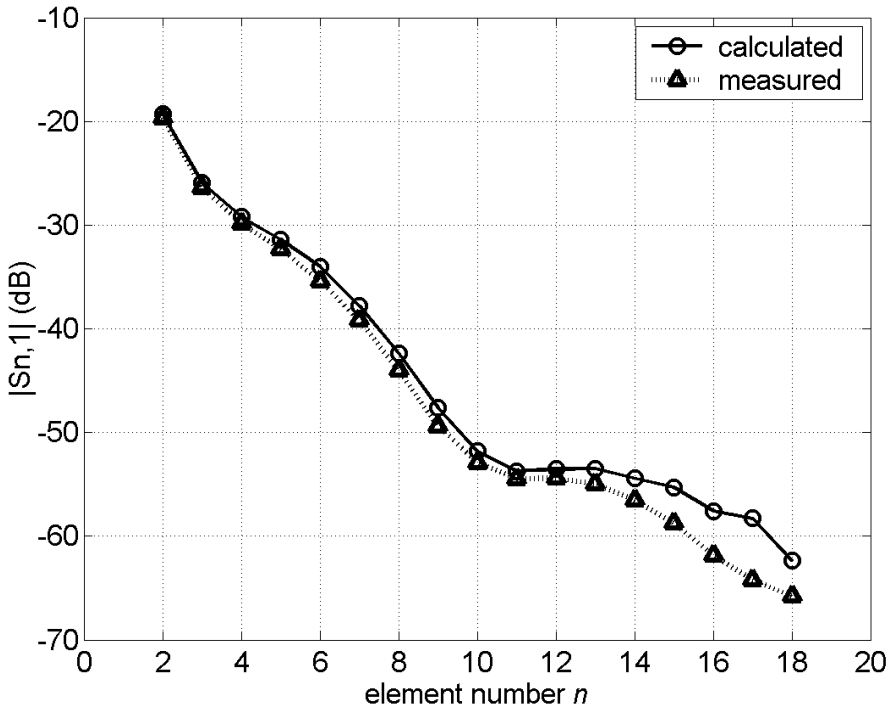

Figure 3.2-K. Array mutual coupling at frequency 5.65 GHz. Radome is present.

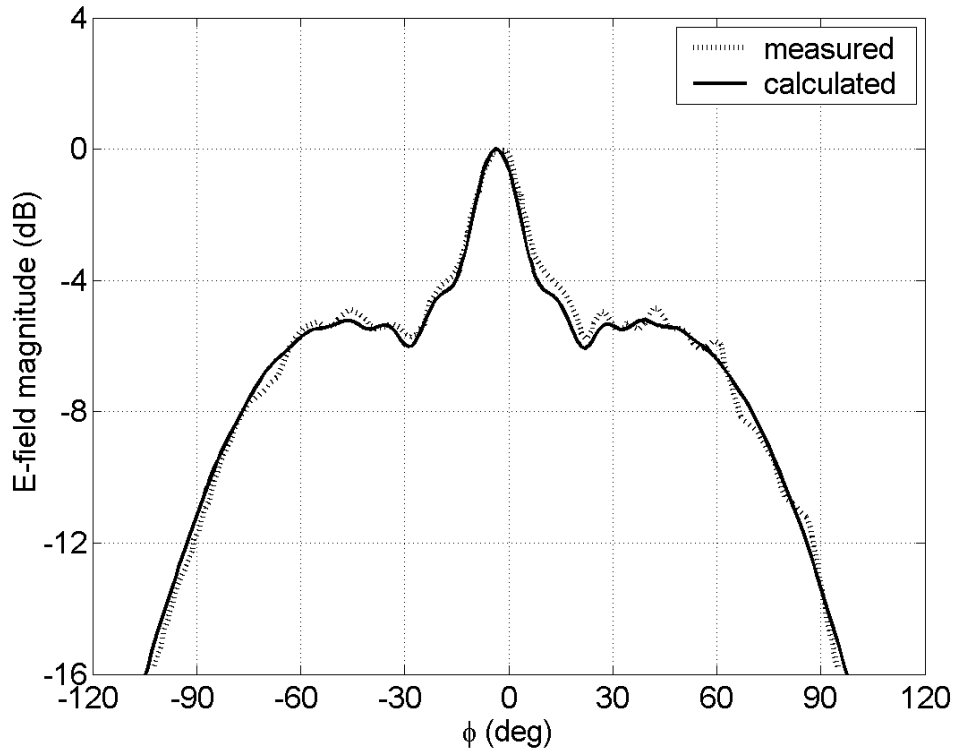

Figure 3.2-L. Embedded (active) element pattern in the E-plane at frequency 5.65 GHz. No radome is present.

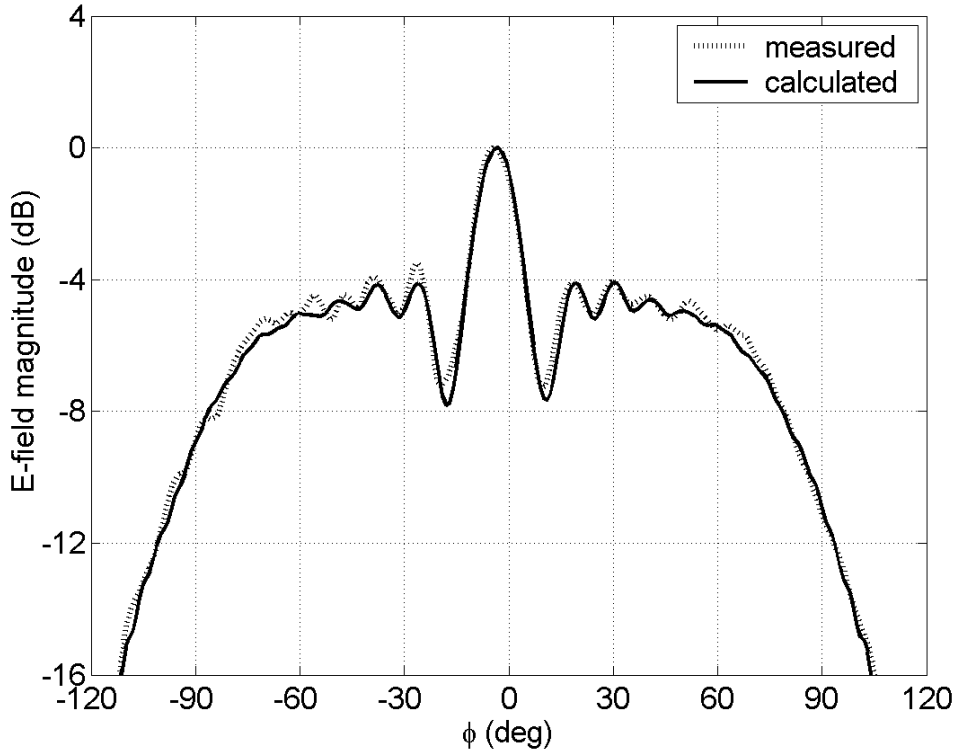

Figure 3.2-M. Embedded (active) element pattern in the E-plane at frequency 5.65 GHz. Radome is present.

6- Computation resources

The simulation has been performed on a PC with the XP Windows operating system. The data relevant to the used computer is given in the Table 3.2-A.

Type of machine	PC Laptop
Number of CPUs	1 Intel Pentium M
CPU Speed	1.3 GHz
RAM	256 MB
OS	Windows XP
CPU time for the full array, mutual coupling included, no radome present (one frequency point)	1 min 12 sec

Table 3.2-A. Properties of the PC used for the simulation

7- Discussion

In the case of the array without radome, the calculations were made by using 5 waveguide modes to represent the field inside the waveguides (the five lowest order waveguide modes, in cut-off order, were used, i.e. in this case TE_{01}, TE_{02}, TE_{10}, TE_{11} and TM_{11}). The results show a very good agreement between the measured and the calculated results.
In the case of the array with radome, during measurements it was not possible to avoid an air-gap between the waveguide apertures and the dielectric cover. This air-gap had an average value of about 0.085 cm, and this value was used in the calculations. There is a very good agreement between the calculated and the measured results up to the 14th element, i.e. down to about -55 dB level (then a small discrepancy occur). The calculations were made using 12 waveguide modes, i.e. we needed more modes to get good convergence of the results compared to the case without dielectric cover.

3.2.4 Simulated results by KTH

1- Entity

Contact person: Patrik Persson
Royal Institute of Technology
Div. of Electromagnetic theory
Teknikringen 31
SE-100 44 Stockholm
Sweden
patrik.persson@ee.kth.se

2- Name of the simulation tool

CADT – Conformal Antenna Design Tool: Program for analysing waveguide-fed apertures on different singly and doubly curved PEC surfaces. A radome can be present for the circular cylinder.

3- Generalities about the simulation tool

CADT is a UTD-MoM based solver for modeling waveguide-fed aperture arrays on different singly and doubly curved surfaces. In particular, the circular, elliptic, hyperbolic and parabolic cylinder, the cone, and the paraboloid. A single layer radome can be added for the circular cylinder. The waveguides can be either rectangular or circular. The tool can calculate the mutual coupling, the radiation patterns (isolated and embedded) and make synthesis analysis (only for singly curved surfaces).

4- Simulation Set-up (Geometry set-up, GUI, mesh, boundary conditions, excitation)

The geometrical structure is described in a mat-file (CADT is mainly written in Matlab), or by using the GUI. The GUI then guides the user throughout the analysis in order to set up the problem, including, among others, the number of rays to be included in the UTD simulation, the number of modes used etcetera. The tool uses as much symmetry as possible, however, for most surfaces (except the circular cylinder) no symmetries exist. Hence, the computation time is increased when consider non-symmetric surfaces.

The radiating boundary conditions are implicitly implemented into the Green's functions. The surfaces are assumed to be infinite in the axial direction. Furthermore, it is assumed that only the dominant mode can propagate inside the waveguides, i.e. all other modes are evanescent. Note that the evanescent modes are considered at discontinuity position, i.e. at the waveguide openings.

5- Simulation results

The results that have been computed are:

1. Mutual coupling, isolated and active (or array mutual coupling).
2. Active element pattern, i.e. radiation pattern of an antenna element in the array environment.

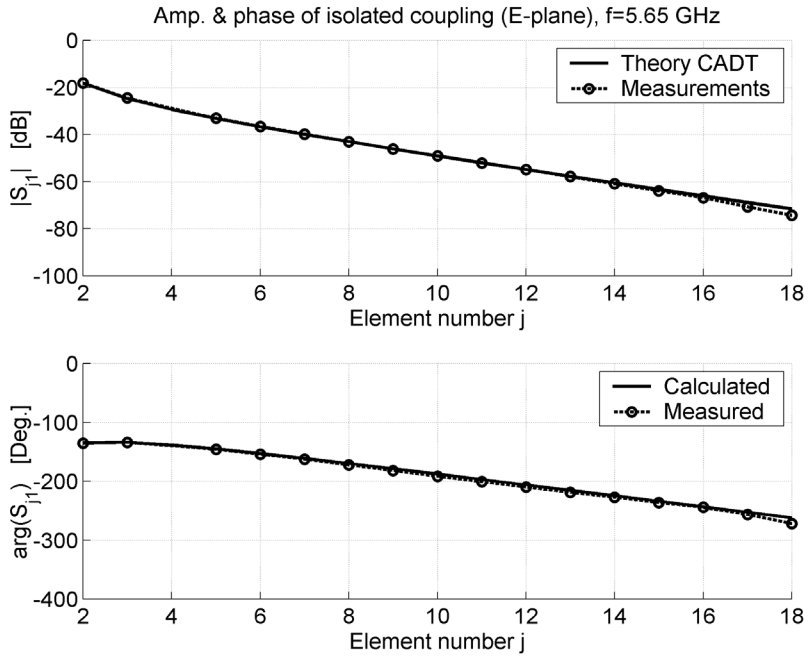

Figure 3.2-L. Isolated mutual coupling at frequency 5.65 GHz. Radome is not present.

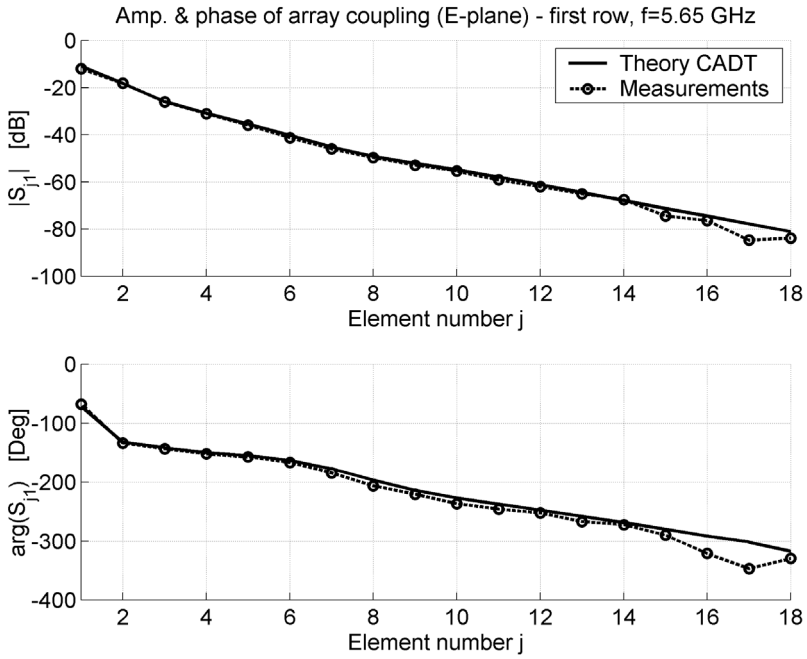

Figure 3.2-M. Active mutual coupling at frequency 5.65 GHz. Radome is not present.

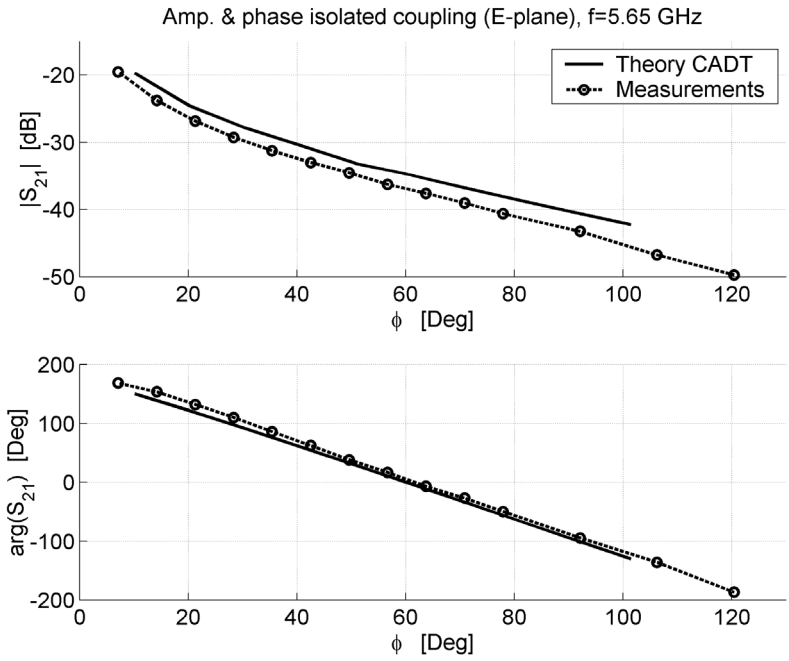

Figure 3.2-N. Isolated mutual coupling at frequency 5.65 GHz. Radome is present. Note, an air gap between the coating the PEC cylinder is not present which is important for accurate results.

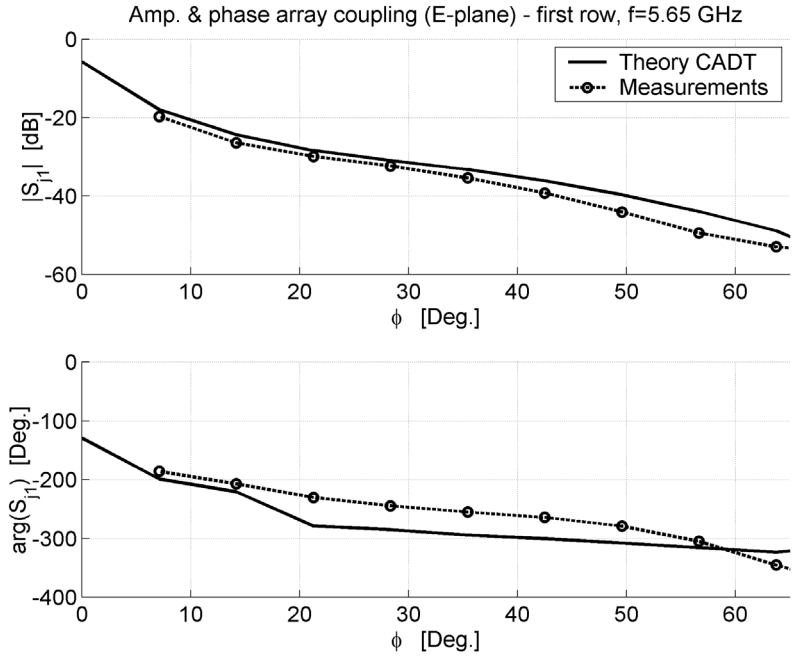

Figure 3.2-O. Active (array) mutual coupling at frequency 5.65 GHz. Radome is present. Note, an air gap between the coating the PEC cylinder is not present which is important for accurate results as shown in the previous section.

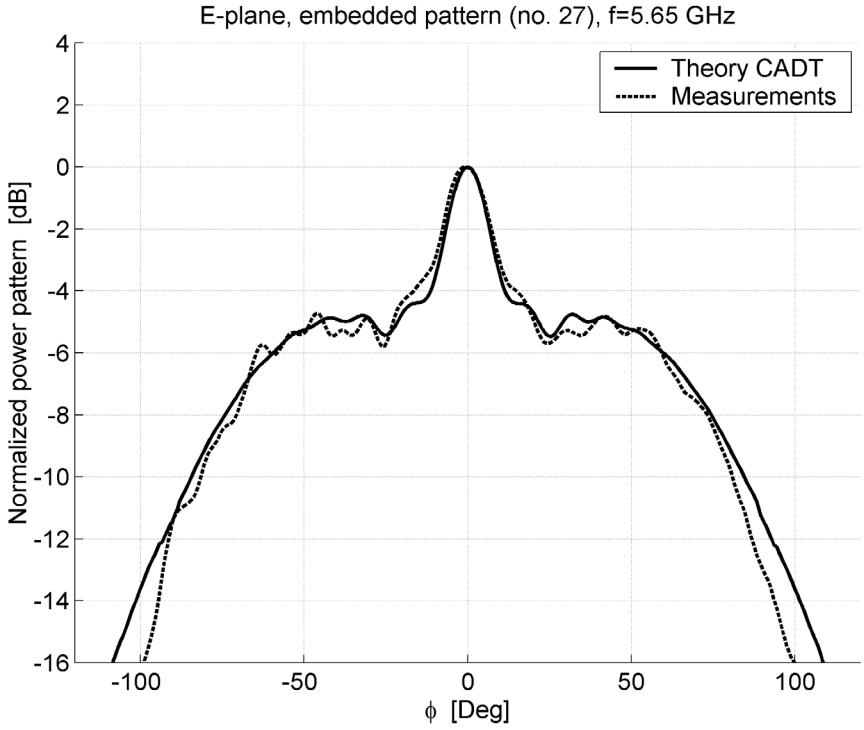

Figure 3.2-P. Active element pattern in E-plane at frequency 5.65 GHz. No radome is present.

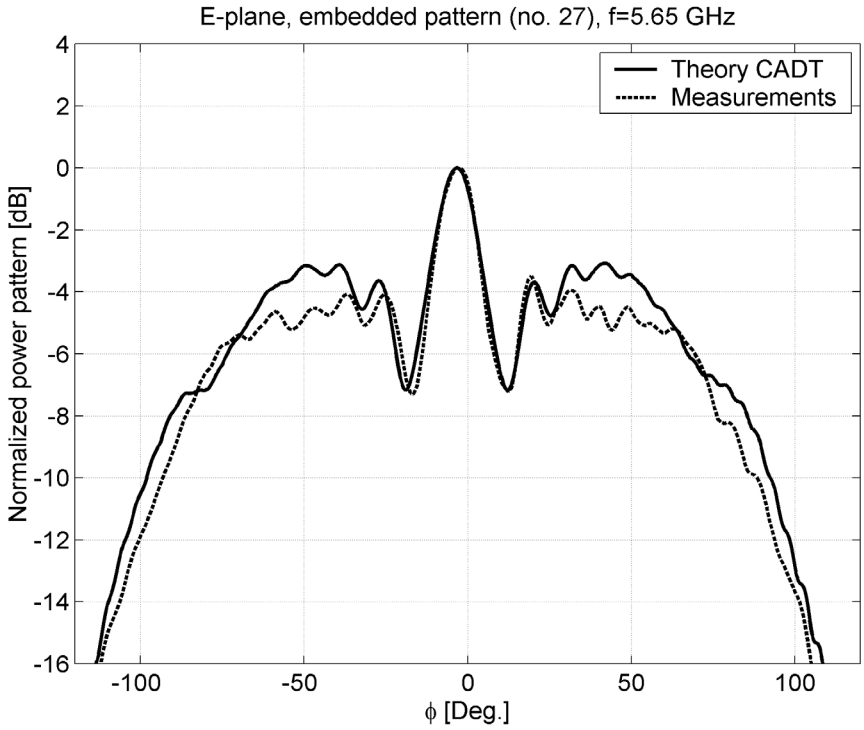

Figure 3.2-Q. Active element pattern in E-plane at frequency 5.65 GHz. Radome is present. Note, an air gap between the coating the PEC cylinder is not present which is important for accurate results as shown in the previous section.

6- Computation ressources

The simulation has been performed on a PC with the XP Windows operating system. The data relevant to the used computer is given in table below.

Type of machine	PC Laptop
Number of CPUs	1 Intel Pentium
CPU Speed	2.4 GHz
RAM	640 MB
OS	Windows XP
CPU time for the full array, mutual coupling, circular cylinder (no coating) (one frequency point)	1 min

Properties of the PC used for the simulation

7- Discussion

In the case of the array without radome, the calculations were made by using 5 waveguide modes to represent the field inside the waveguides (the five lowest order waveguide modes, in cut-off order, were used, i.e. in this case TE_{01}, TE_{02}, TE_{10}, TE_{11} and TM_{11}). The results show a very good agreement between the measured and the calculated results. For the case with a radome present there was not possible to avoid an air-gap between the waveguide apertures and the dielectric cover. This air-gap had an average value of about 0.085 cm, and this value was *not* used in the calculations – it cannot be included in the asymptotic formulation. Hence, the agreement is not as good as for the non-coated case. The calculations were made using 12 waveguide modes, i.e. we needed more modes to get good convergence of the results compared to the case without dielectric cover.

3.3 Structure 2: Cylindrical sector microstrip antenna (ϕ polarization)

3.3.1 Structure description

1- Entity

Michael Thiel Michael.Thiel@dlr.de
DLR +49 8153 28-3071
Oberpfaffenhofen +49 8153 28-2328
82234 Wessling
Germany

2- Structure Definition

Single layer cylindrical sector microstrip antenna
phi-polarised
direct fed

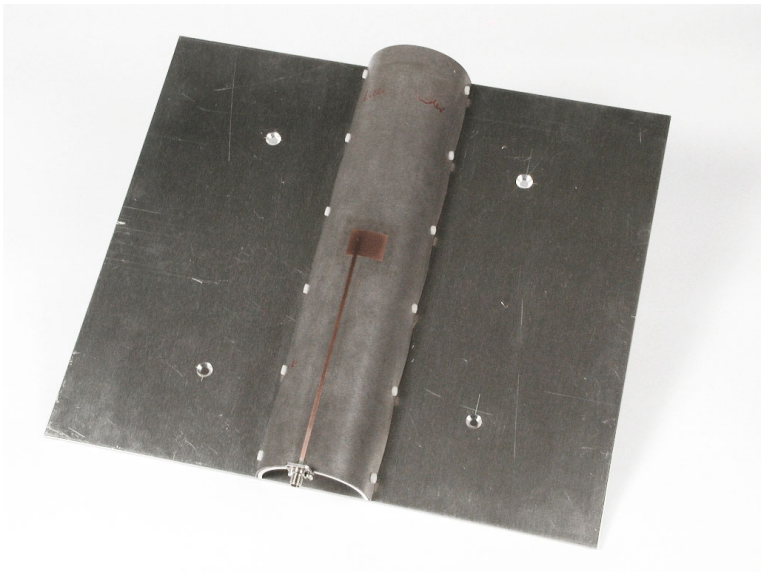

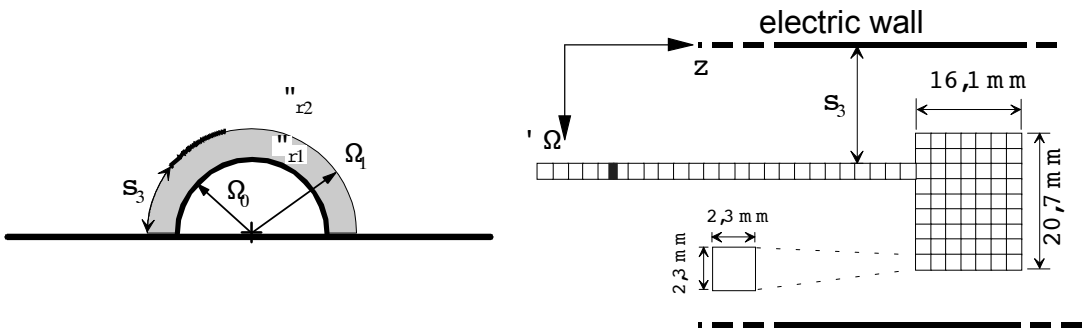

Figure 3.3-A. f_0=4,4 – 5,0 GHz, ρ_0= 30,0 mm, ρ_1= 30,787 mm, ε_{r1}= 2,33, ε_{r2}= 1,0, s_3 chosen so that patch in middle of half cylinder between walls.

3- Expected results

4- Interest of the structure

Special conformal shape, partly found on airframes. May be used for specific base station applications or if certain requirements for illumination of half spaces are needed.

Modelling of gap source necessary (or wave port), not by probe feeding.
Modelling of thin layers necessary. Special dyadic Green's function needed to take into account the electric walls.

5- Keywords

Cylindrical sector, microstrip antenna, linear polarised, phi-polarised.

6- References

Results are given in [1]. Theory for derivation of the Green's function is described in [2]. The dyadic Green's function is used for integral equation solution in spectral domain.

[1] M. Thiel, Die Analyse von zylinderkonformen und quasi-zylinderkonformen Antennen in Streifenleitungstechnik, Forschungsbericht DLR-FB 2002-25, (Dissertation, TU München), 2002.

[2] M. Thiel and A. Dreher, "Dyadic Green's Function of Multilayer Cylindrical Closed and Sector Structures for Waveguide, Microstrip-Antenna and Network Analysis", *IEEE Trans. Microwave Theory Tech.*, vol. 50, pp. 2576-2579, Nov. 2002.

3.3.2 Structure measurements

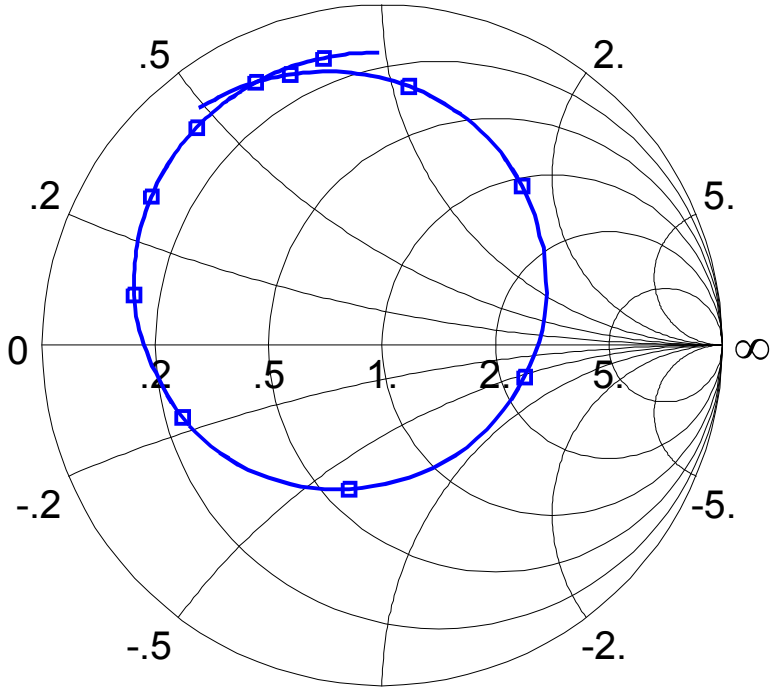

Figure 3.3-B. Measured input impedance 4,4-5,0GHz (--□--)

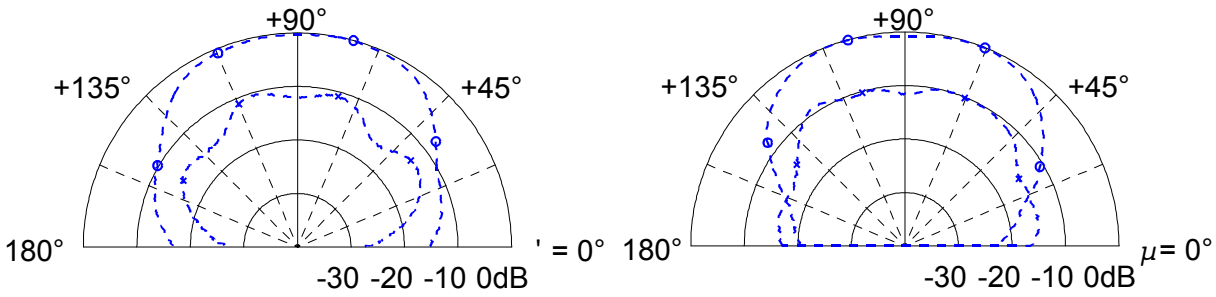

a) b)

Figure 3.3-C. Far field measurements
a) E-plane: Measurement (- -○- -)
b) H-plane: Measurement (- -○- -)

3.3.3 Simulated results by DLR

7- Applicability

The solution in above references is done with integral equation in spectral domain in combination with method of moment solution. Rooftop basis functions are used with Galerkin's method. The

boundary value problem of the layered structure is solved by the analytical derivation of the dyadic Green's function in spectral domain. This is derived for the special case of electric walls included.

The software MCAT was developed at DLR for this purpose:

Cylindrical (sector and closed) and quasi-cylindrical simulation software for single layer microstrip structures. The Green's function can be used for arbitrarily layered, also aperture coupled structures. Simulation results are: surface currents, input impedance, far fields, mutual coupling parameters.

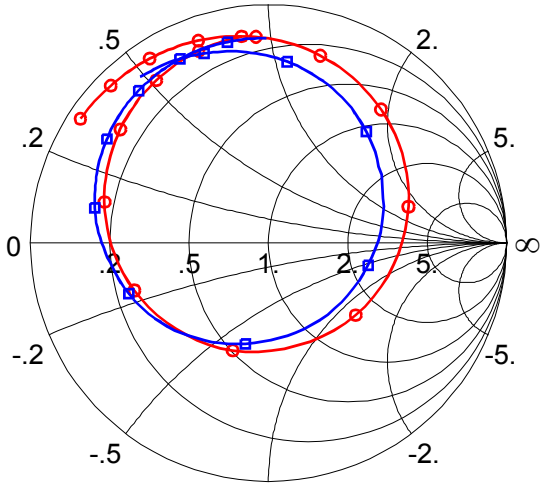

Figure 3.3-D. Input impedance, simulation (--○--), measurement (--□--)

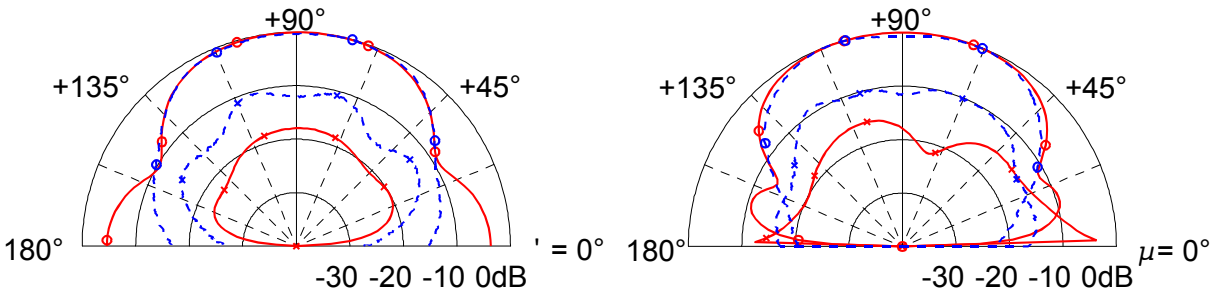

Figure 3.3-E. Far field

a) E-plane: Simulation (—○—), measurement (- -○- -)

b) H-plane: Simulation (—○—), measurement (- -○- -)

8- Confidentiality

3.3.4 Simulated results by CHALMERS and University of Zagreb

1- Entity

Contact person: Zvonimir Sipus
Chalmers University of Technology
Department of Electromagnetics
SE-412 96 Gothenburg
Sweden
e-mail: zvonimir@elmagn.chalmers.se

2- Name of the simulation tool

G1DMULT - Program for analyzing conformal microstrip and waveguide arrays

3- Generalities about the simulation tool

G1DMULT is an IE-MoM based solver for modeling microstrip patch arrays and waveguide arrays embedded in circular-cylindrical or spherical multilayer structures. It is assumed that the patches or waveguides have rectangular shape, and three types of feeding structure are considered for microstrip patch antennas: microstrip transmission line, coaxial transmission line and aperture coupling.

4- Simulation Set-up (Geometry set-up, GUI, mesh, boundary conditions, excitation)

The geometrical structure was described in an input text file. Since the structure posses spherical symmetry and since the radiating structure (microstrip patches) has a simple rectangular shape, the antenna can be described with a few parameters.

There is no need for mashing since the program uses the entire-domain basis functions.

The software assumes that the dielectric layers and grounded planes completely follow the cylindrical or spherical symmetry (e.g. the cylindrical structure is infinite in the axial direction). The radiating boundary conditions are implicitly implemented into the Green's functions; the metal parts are modelled by PEC boundary conditions. The feed (the coaxial probe) is modeled as a filament of constant current. A radial attachment function is included into the feed model in order to ensure the continuity of the current at the junction between the probe and the patch. No additional geometry is required by a simulator. The program almost immediately inputs the geometry and sets up the rest of simulations.

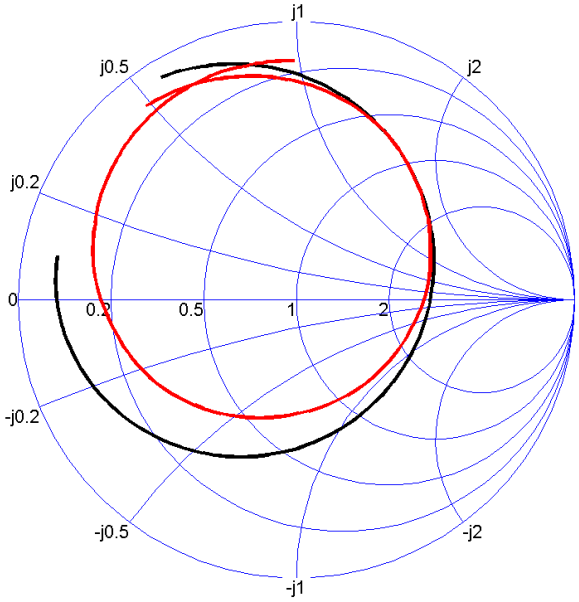

Figure 3.3-F. Input impedance, simulation (——), measurement (——)

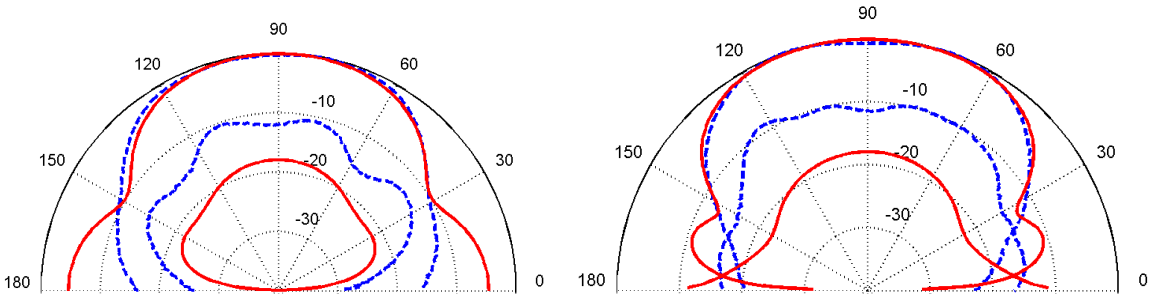

Figure 3.3-G. Far field

a) E-plane: Simulation (——), measurement (- -- -)

b) H-plane: Simulation (——), measurement (- -- -)

3.4 Structure 3: Spherical patch antenna

3.4.1 Structure description

1- Entity

Contact person: Zvonimir Sipus
Chalmers University of Technology
Department of Electromagnetics
SE-412 96 Gothenburg
Sweden
e-mail: zvonimir@elmagn.chalmers.se

2- Name of the structure

Conformal spherical patch array

3- Generalities

Spherical arrays present a natural choice if complete hemispherical coverage with nearly constant beam is needed. Microstrip patch antennas can be easily made to conform to the structure and they are often used because of their thin profile, light weight and low cost. Therefore, one possible and simple realization of a spherical array is to use patch elements on a spherical supporting structure.

4- Structure Description

The spherical patch array is built from a copper sphere of radius a = 18.7 cm at which patch antennas are mounted. The selected dimensions of the patches are 5.1 $\times$ 5.1 cm^2, and the small styrofoam cubes of 0.52 cm thickness are used as spacers between patches and grounded shell (therefore ε_r = 1.0). Each patch is connected with the SMA connector, and the distance of the feed point from the patch center is 1.95 cm. Three patches are mounted on the grounded sphere to test mutual coupling in E-plane: the central one and two side patches. The distance between the central patch and side patches are 10.25 cm and 20.5 cm, respectively. This distance is measured as an arc length at the grounded tube between SMA connectors. The structure is fed by a 50 Ω coaxial line.

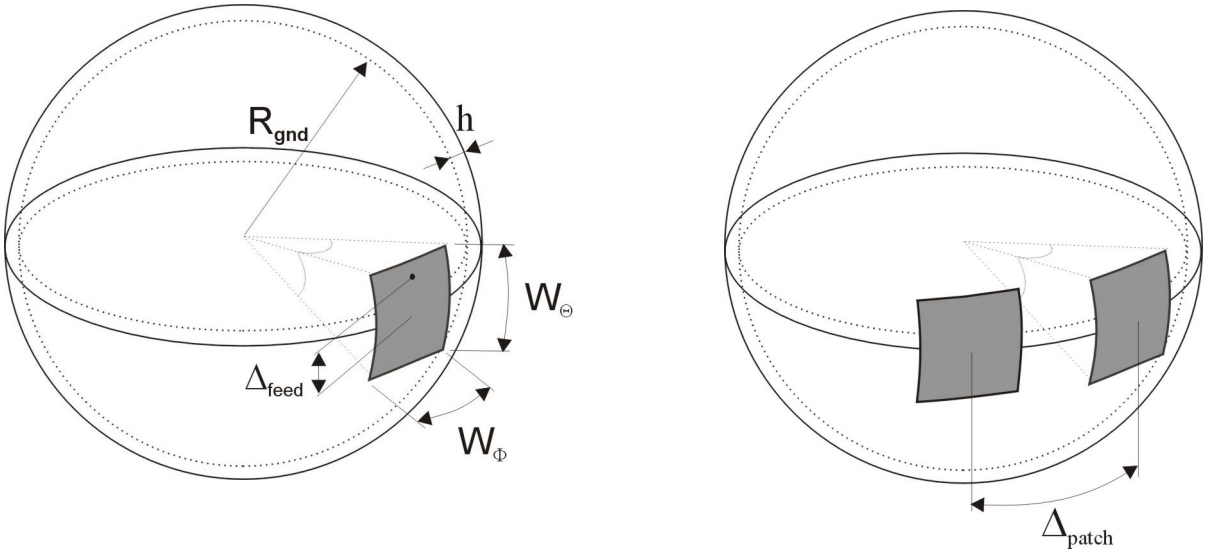

Notation	Dimension
R_{gnd}	18.7 cm
ε_r	1.0
h	0.52 cm
W_θ	5.1 cm
W_ϕ	5.1 cm
Δ_{feed}	1.95 cm
Δ_{patch} (first case)	10.25 cm
Δ_{patch} (second case)	20.5 cm

Figure 3.4-A. The developed spherical array.

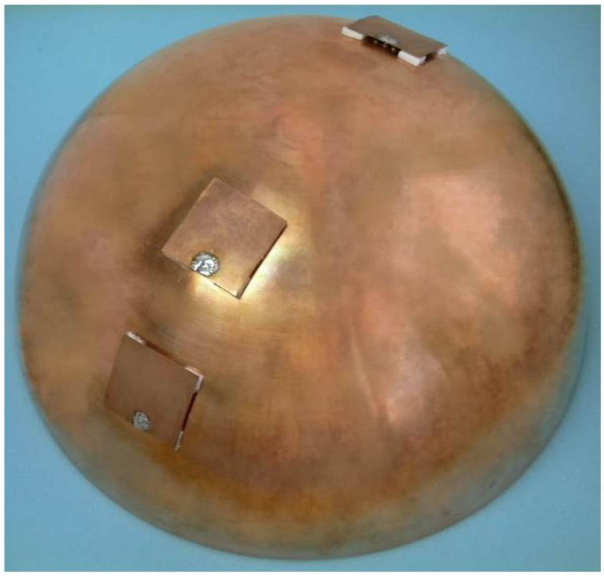

Figure 3.4-B. Photo of the developed spherical array.

3.4.2 Structure measurements

We have measured:

1. S_{21} parameter between two patches placed in E-plane (Δ_{patch} = 10.25 cm in case 1; Δ_{patch} = 20.5 cm in case 2). The reference plane was at the grounded sphere, the working frequency was between 2 and 3 GHz.
2. S_{11} parameter of one patch. The reference plane was at the grounded sphere, the working frequency is between 2 and 3 GHz
3. Radiation pattern of one patch in E- and H-plane. The working frequency was 2.5 GHz.

An example of the measured S_{21} parameter is given in the following picture.

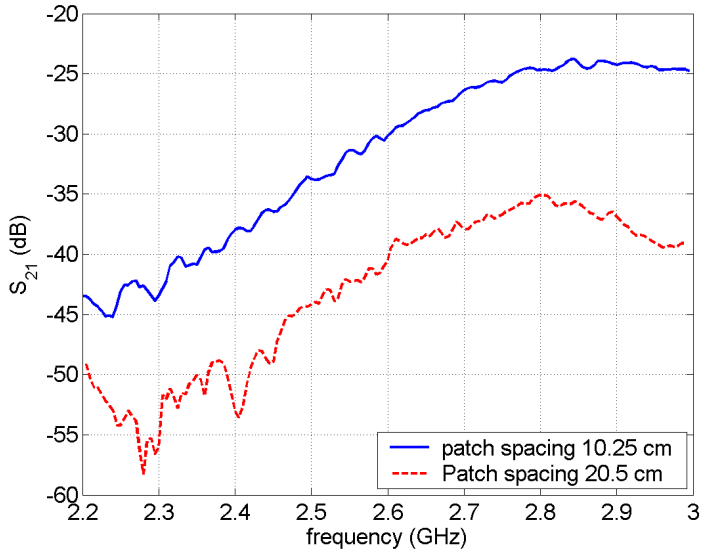

Figure 3.4-C. Measured mutual coupling coefficients of two patches in E-plane as function of frequency and spacing between patches; patch spacing : 10.25 cm and 20.5 cm .

An example of the measured input impedance of a single patch is given in the following picture. Input impedance is determined from the S_{11} parameter, and the reference plane is at the grounded sphere.

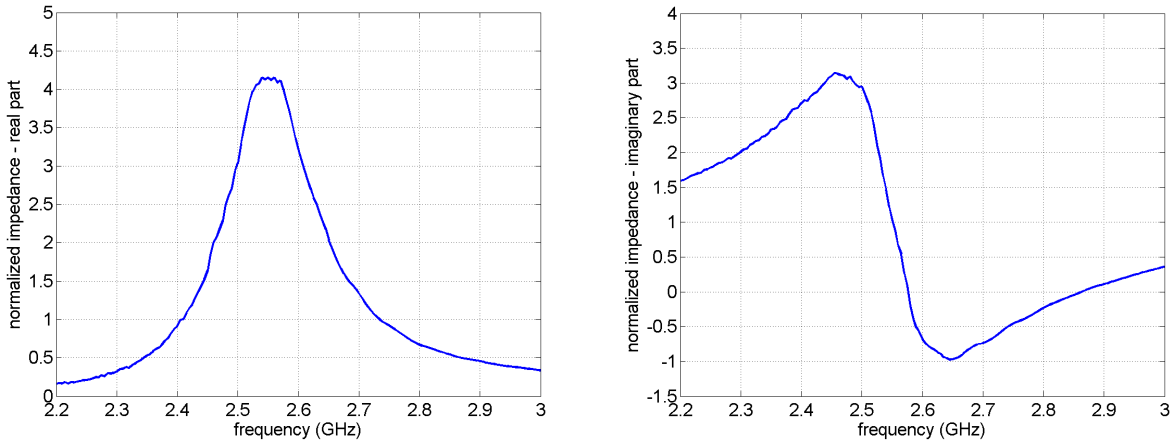

(a) (b)

Figure 3.4-D Measured input impedance; (a) real part, (b) imaginary part.

An example of the measured radiation pattern at 2.5 GHz in *E*- and *H*-plane is given in the following picture.

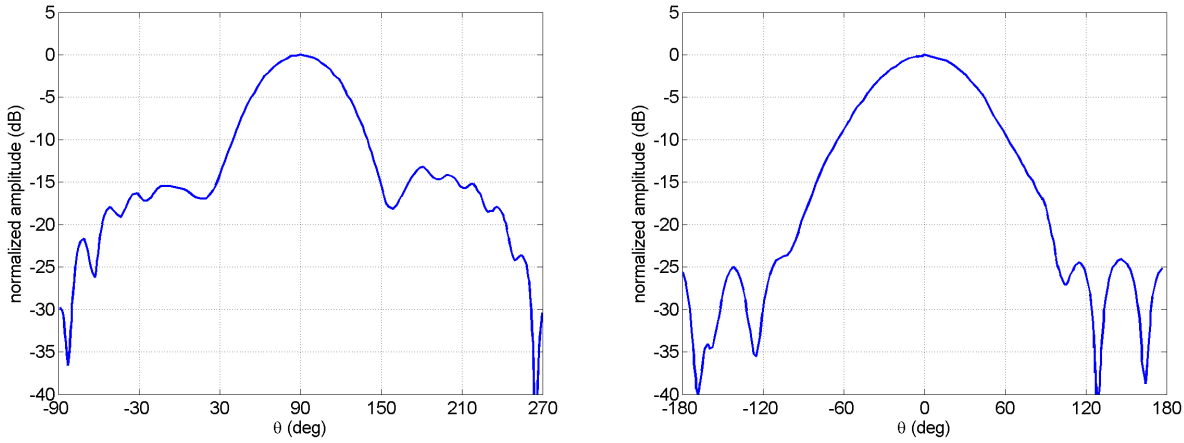

(a) (b)

Figure 3.4-E. Radiating pattern of spherical-rectangular patch antenna: (a) E-plane, (b) H-plane.

3.4.3 Simulated results by CHALMERS and University of Zagreb

1- Entity

Contact person: Zvonimir Sipus
Chalmers University of Technology
Department of Electromagnetics
SE-412 96 Gothenburg
Sweden
e-mail: zvonimir@elmagn.chalmers.se

2- Name of the simulation tool

G1DMULT - Program for analyzing conformal microstrip and waveguide arrays

3- Generalities about the simulation tool

G1DMULT is an IE-MoM based solver for modeling microstrip patch arrays and waveguide arrays embedded in circular-cylindrical or spherical multilayer structures. It is assumed that the patches or waveguides have rectangular shape, and three types of feeding structure are considered for microstrip patch antennas: microstrip transmission line, coaxial transmission line and aperture coupling.

4- Simulation Set-up (Geometry set-up, GUI, mesh, boundary conditions, excitation)

The geometrical structure was described in an input text file. Since the structure posses spherical symmetry and since the radiating structure (microstrip patches) has a simple rectangular shape, the antenna can be described with a few parameters.

There is no need for mashing since the program uses the entire-domain basis functions.

The software assumes that the dielectric layers and grounded planes completely follow the cylindrical or spherical symmetry (e.g. the cylindrical structure is infinite in the axial direction). The radiating boundary conditions are implicitly implemented into the Green's functions; the metal parts are modelled by PEC boundary conditions. The feed (the coaxial probe) is modeled as a filament of constant current. A radial attachment function is included into the feed model in order to ensure the continuity of the current at the junction between the probe and the patch. No additional geometry is required by a simulator. The program almost immediately inputs the geometry and sets up the rest of simulations.

5- Simulation results

The results that have been computed are:

1. Input impedance at input port
2. Mutual coupling between two antenna elements
3. Radiation pattern of a single patch antenna.

The comparison of calculated and measured input impedance of a single patch is given in Fig. 3.4-F. Input impedance is determined from the S_{11} parameter (a normalization impedance is 50 Ω), and the reference plane is at the grounded sphere. S_{21} parameter between two patches for two different distances between patches is considered in Fig. 3.4-G. The comparison of calculated and measured radiation pattern in both E- and H-planes is given in Fig. 3.4-H. Notice that in the measured radiation pattern the maximum value is taken as the reference value.

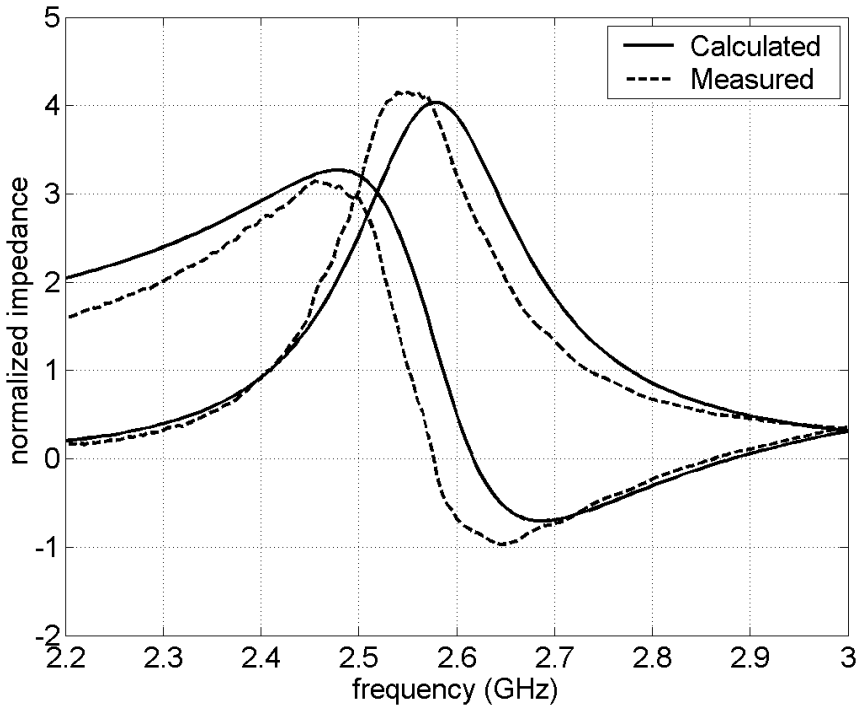

Figure 3.4-F. The comparison of calculated and measured input impedance of the spherical patch antenna.

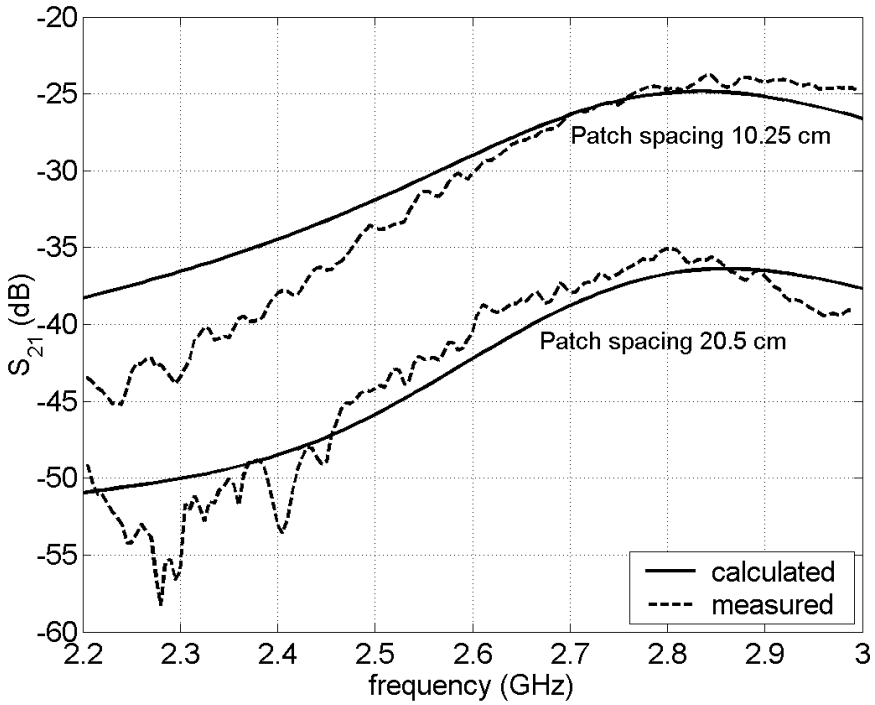

Figure 3.4-G. Comparison of calculated and measured mutual coupling coefficient of two patches in E-plane as function of frequency and spacing between patches.

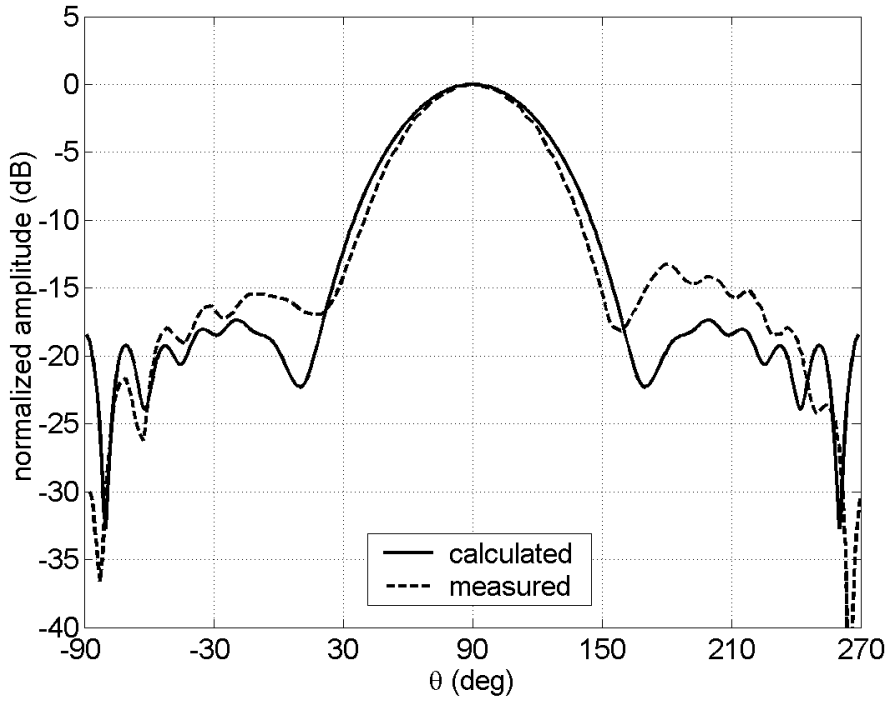

(a)

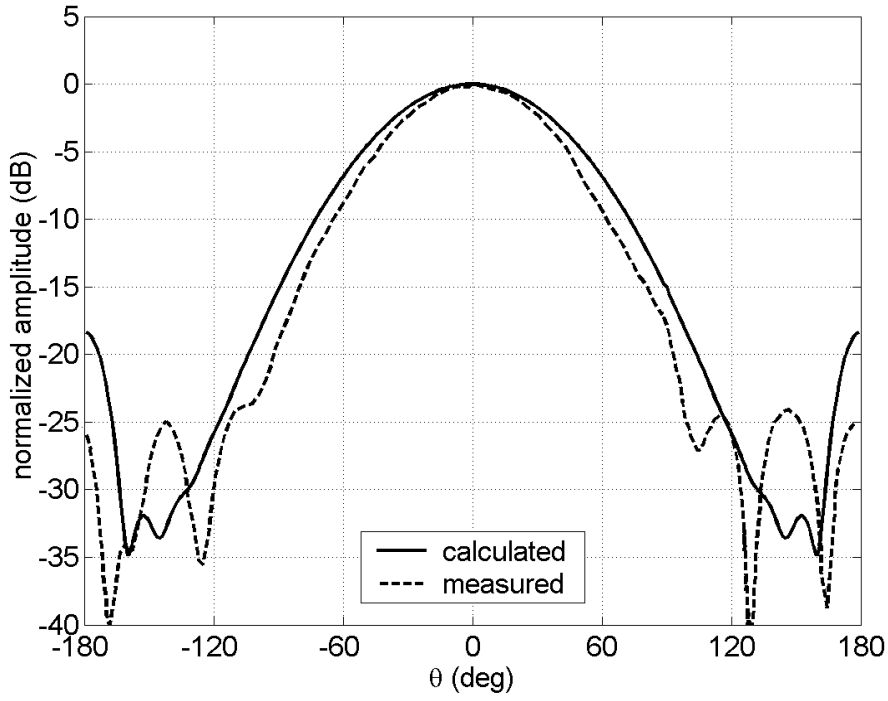

(b)

Figure 3.4-H. Radiating pattern of a spherical-rectangular patch antenna: (a) E-plane, (b) H-plane.

6- Computation ressources

The simulation has been performed on a PC with the XP Windows operating system. The data relevant to the used computer is given in the Table 3.4-A.

Type of machine	PC Laptop
Number of CPUs	1 Intel Pentium M
CPU Speed	1.3 GHz
RAM	256 MB
OS	Windows XP
CPU time	2 min 59 sec
Averaged CPU time per 1 frequency point	4.37 sec

Table 3.4-A. Properties of the PC used for the simulation

The simulation is performed over 41 discrete frequency points in the range 2.0 – 3.0 GHz. The needed CPU time was 2 min and 59 sec, i.e. the averaged CPU time per one frequency point was 4.37 seconds. If only one frequency point was used in calculations, the needed CPU would be 15 sec.

7- Discussion

The simulated structure was easy to set up due to the rectangular shape of the patch antennas and due to the regular spherical structure. The simulation results were obtained after obtaining the measured results. Although the program assumes regular shape of the patch antennas and of the structure, we believe that the program is useful in designing conformal antennas: the first design can be done with fast solver for conformal antennas like G1DMULT, and the details can be designed with a general EM solver.

3.4.4 Simulated results by DLR

1- Computed results by DLR:

DLR developed a software code which is based on MoM to analyse microstrip antennas on spherical multilayered closed and hemispherical structures.

The comparison of the calculated input impedance by DLR software (of the single patch antenna mentioned in section 4), the result by EMSS-Feko, and the measurement is shown in Figure 6.

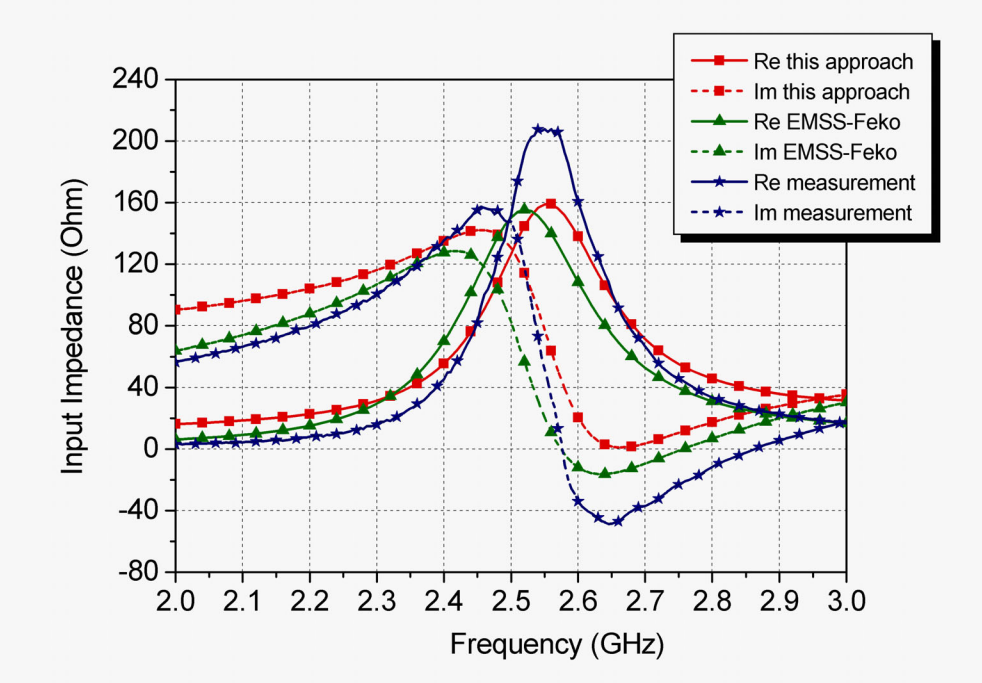

Figure 3.4-I. Comparison of the calculated input impedance by DLR software, Feko code and measurement.

2- Literature

[1] Z. Sipus, N. Burum, and J. Bartolic, "Analysis of rectangular microstrip patch antennas on spherical structures," *Microwave and Optical Technology Letters,* Vol. 36, pp. 276-280, Feb. 2003.

[2] N.Burum, Z. Sipus, and J. Bartolic, "Mutual coupling between spherical-rectangular microstrip," *Microwave and Optical Technology Letters,* Vol. 40, pp. 387–391, Mar. 2004.

[3] EM Software & Systems – S.A. (Pty) Ltd, Stellenbosch, South Africa, *FEKO – Field Computations Involving Bodies of Arbitrary Shape*, 2003, http:/www.feko.info

4 HYBRID SPECTRAL DOMAIN-UTD METHOD

Zvonimir Sipus, *CHALMERS*
Patrik Persson, *KTH*

4.1 Introduction

The purpose of this chapter is to present the hybrid spectral domain – UTD method for analyzing conformal antennas (UTD – Uniform Theory of Diffraction). The described method is a result of structuring the research on conformal antennas in Europe, i.e. the developed method is a result of joining research activities of CHALMERS, KTH and University of Zagreb, Croatia. The basic idea behind the hybrid method is to combine different analysis methods for conformal antennas and, at the same time, preserve the advantages of the considered methods.

Possible design guidelines of conformal antennas can be demanded aerodynamic or hydrodynamic considerations, coverage reasons or aesthetic reasons. For example, future antenna systems will have a variety of beamforming and beamsteering capabilities. Arrays on cylindrical structures offer a possibility either to create directed beams in arbitrary directions, or to cover 360 degrees in the horizontal plane. This is useful also in radar systems mounted on aircraft and missiles.

The abilities of the hybrid spectral domain – UTD method will be demonstrated on circular cylindrical arrays of waveguide elements. A common technique for analysing circular cylindrical structures is to use a modal expansion approach together with the moment method, i.e. to transform the three-dimensional problem into a spectrum of one-dimensional problems (see e.g. [1]). In more details, the problem of determining the E- and H-fields radiated by a source embedded in a planar, cylindrical or spherical structure can be simplified if we perform the two-dimensional (2D) Fourier transformation in the coordinates for which the structure is homogeneous. In the cylindrical case, we perform the Fourier transformation in the axial direction and the Fourier series in the ϕ direction [1]. For each spectral component of the source, the excited electromagnetic field in two directions, for which the structure is homogeneous, has the same harmonic variation as the source. As a result, only the electromagnetic field variation in the normal direction of the cylinder is unknown. In other words, our original three-dimensional problem is transformed into a spectrum of one-dimensional problems, which is much easier to solve. Following the same principle one can develop a numerical algorithm for calculating Green's functions in the spectral domain. One possibility is to use the G1DMULT algorithm [2].

Earlier, several authors have used a modal approach to study the radiation of slots on a circular cylinder covered by a single-layer dielectric radome. For example, Steward and Goldman studied finite arrays of rectangular waveguides [3], Hessel and Sureau studied infinite arrays of axial slits [4], and Balzano studied an infinite array of circular waveguides [5]. Recently, the interest for antenna systems with a variety of beamforming and beamsteering capabilities renews the research of finite waveguide arrays [6]. In this study the spectral domain method (G1DMULT) was used. Unfortunately, there are two drawbacks of this approach when applied to finite arrays; (i) the number of required modes in the Fourier series increases with increasing cylinder radius (which may cause numerical difficulties), (ii) there is a need for calculating highly oscillating integrals in the moment method when there is a large axial separation of the slots. There are a lot of techniques to accelerate the inverse Fourier transformation/series, see e.g. [7], [8]. Other possibilities are to use the residue series expansion [3], [4], or to apply a high-frequency technique like the UTD method

[9]-[13]. However, neither of these two methods is suitable for analysing cylindrical structures with multilayer dielectrics.

Using an asymptotic, high-frequency, method is favourable when the dimensions of the structure of interest is large in terms of wavelengths. One example of such an approach is the UTD which can be used to analyse problems that are otherwise numerically too complex. The UTD is an extension of the classical geometrical optics (GO) (direct, reflected and refracted rays), and it overcomes limitations of GO by introducing diffraction mechanism. The structure size is not a serious limitation since the minimum radius of curvature of the surface can be quite small. A commonly used rule is that $kR \geq 2-5$ for accurate results (k is the wave number, R is the radius of the cylinder) [14]. Unfortunately, there is no complete high frequency solution for dielectric coated surfaces yet available. For dielectric-coated cylindrical structures there is only a solution for single-layer cylindrical structure [12], [13]. Therefore, the idea was to develop the method that will use advantages of the spectral domain method (possibility of analysing multilayer structures) and of the UTD (possibility of analysing electrically large structures).

4.2 Description of the method

The goal with the developed hybrid method is to reduce the number of terms in the Fourier series and to reduce the length of integration in the Fourier transformation. The basic idea is to subtract the asymptotic part of the Green's function, and to calculate the asymptotic part using UTD [9], [10]. To shortly illustrate the method we will consider a waveguide array embedded in multilayer dielectric structure. Equation (4.1) shows the expression for the mutual admittance between two apertures. This is in fact the ij^{th} element in the moment method matrix, see [15] for more details about the formulation of the moment method.

$$Y_{ij} = \frac{1}{4\pi^2}\sum_{-\infty}^{\infty}\int_{-\infty}^{\infty}\tilde{M}_i(-m,-k_z)\overline{\overline{\tilde{G}}}(m,k_z,)\tilde{M}_j(m,k_z)dk_z. \tag{4.1}$$

After subtracting the asymptotic part we get the following two parts to be computed:

$$\begin{aligned} Y_{ij} &= \frac{1}{4\pi^2}\cdot\sum_{-\infty}^{\infty}\int_{-\infty}^{\infty}\tilde{M}_i(-m,-k_z)\cdot\left[\overline{\overline{\tilde{G}}}(m,k_z)-\overline{\overline{\tilde{G}}}_{asym}(m,k_z)\right]\cdot\tilde{M}_j(m,k_z)dk_z \\ &+ \int_{\substack{test\\function}}\int_{\substack{basis\\function}} M_i(\phi,z)\overline{\overline{G}}_{asym}(\phi-\phi',z-z')\cdot M_j(\phi',z')dS'dS \end{aligned} \tag{4.2}$$

The first term in eq. (4.2) is calculated using the spectral-domain approach, while the second term is calculated using UTD. However, one still needs to select a suitable $\overline{\overline{\mathbf{G}}}_{asym}$. Since UTD cannot handle multilayered structures [12], [13] we have decided to choose the Green's function as that of a source placed in a homogeneous media close to a grounded PEC tube. The permittivity of the homogeneous media is select as the average value of the two layers enclosing the source. That is, if the nearby layer with $\rho \leq \rho_{source}$ and the nearby layer with $\rho \geq \rho_{source}$ have the same permittivity we select that permittivity for the homogeneous media. Since the source in our case is an infinitesimal magnetic dipole placed at the grounded tube, we will use the permittivity of the first dielectric layer above the grounded tube as permittivity of the homogeneous media for $\overline{\overline{\mathbf{G}}}_{asym}$. Therefore, the proposed method combines robustness of the spectral approach (i.e. the possibility of analysing multilayer structures), and simplicity of the UTD method.

4.3 Accuracy of the hybrid spectral domain – UTD method

An array of 18x3 rectangular waveguide apertures was built at Ericsson Microwave Systems AB, Mölndal, Sweden ([10]; see Figs. 4-A and 4-B).

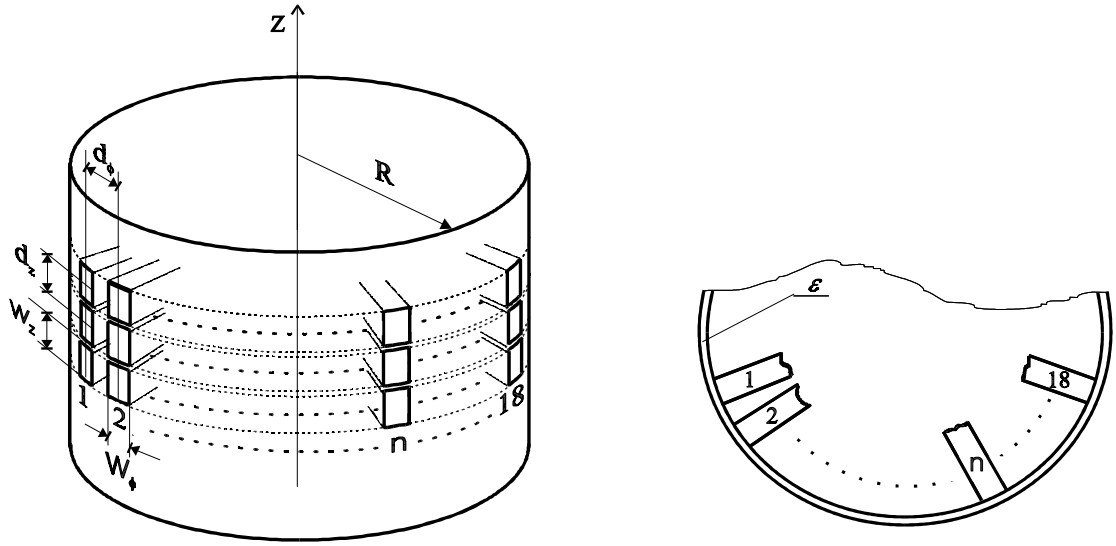

(a) (b)

Figure 4-A. Circular-cylindrical array of waveguide elements.
(a) sketch of the array , (b) cross-section.

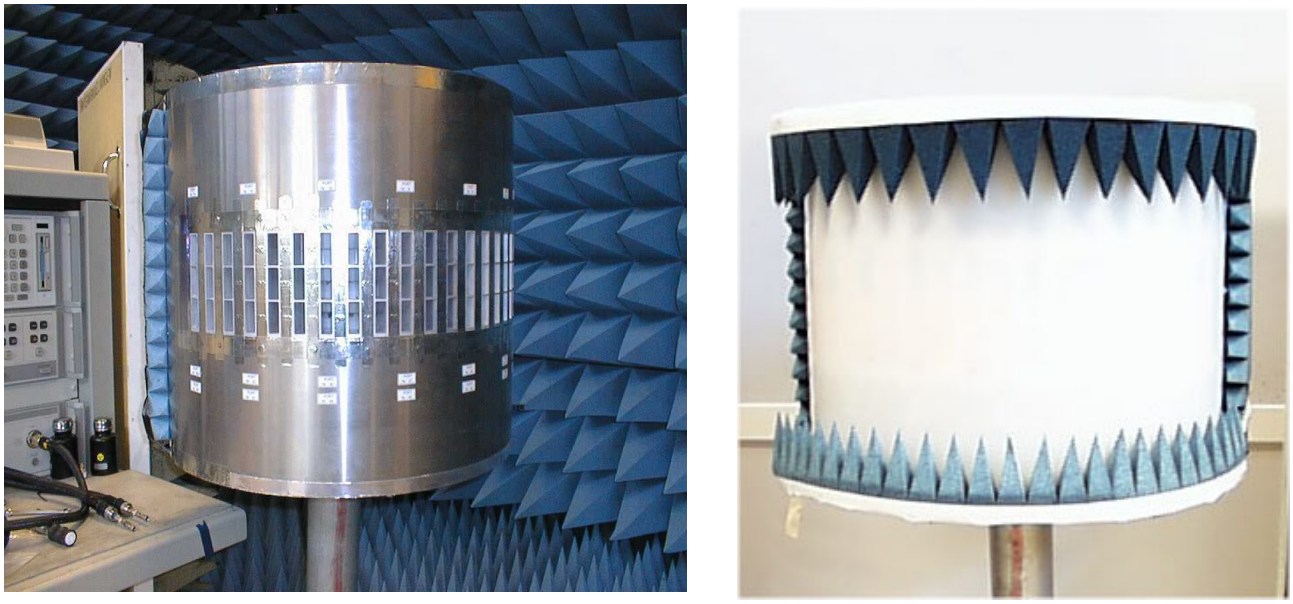

(a) (b)

Figure 4-B. Ericsson test model.
a) without dielectrical radome, b) with dielectrical radome

The radius of the cylinder is 30 cm (5.65λ at the operating frequency 5.65 GHz), and each row of waveguide elements in the ϕ-direction corresponds to an angular interval of approximately 120 degrees. The waveguide aperture dimensions are W_ϕ = 1.6 cm, W_z = 3.9 cm, d_ϕ = 3.708 cm, d_z = 4.1 cm and they are all terminated with their characteristic impedance. The array is then covered with a radome. The thickness is 0.399 cm, the dielectric constant ε_r = 2.32 and $\tan\delta$ = 0.000247. Furthermore, it was not possible to avoid an air-gap between the PEC cylinder and the dielectric coating. The average value of the air-gap is equal to 0.085 cm (this air-gap is included in the simulations). In order to minimize the edge effects, absorbers were placed at the edges of the array as seen in Fig. 4-B-b. All calculations were made using 12 waveguide modes to represent the field inside the waveguides, and ε_r = 1.0 was selected for $\bar{\bar{\mathbf{G}}}_{asym}$, although the air-layer is very thin.

The developed method has been verified against both measurements and calculated results obtained with the approach used in [6] where no acceleration techniques were used. In Fig. 4-C the comparison of the calculated and measured S-parameters is shown for the first row of waveguide elements, i.e. we plotted $S_{n,1}$, n=2,18. The results show a good agreement between the measured and the calculated results, both in amplitude and phase. Note that the hybrid method presented here gives almost identical results as the approach in [6]. But the hybrid method is much faster and we have used 10 times less modes in the inverse Fourier series and 20 times shorter length of integration in the inverse Fourier transformation (see eqs. (4.1) and (4.2)).

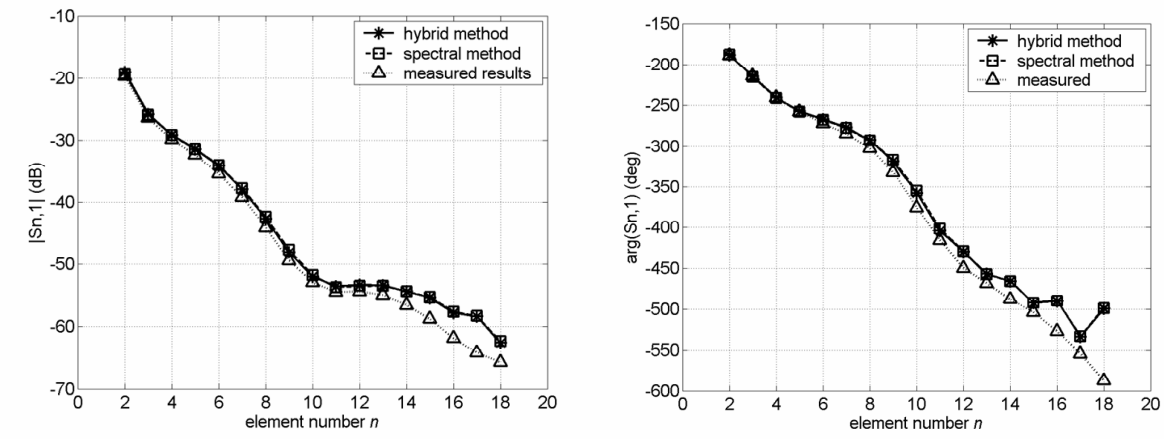

(a) (b)

Figure 4-C. The mutual coupling in the E-plane for the array of waveguide elements. (a) amplitude, (b) phase.

In Fig. 4-D the embedded element pattern for the center element of the array (element no. 27) is shown in the azimuthal plane. Once again calculations and measurements agrees very well. It can be noticed that the shape of the element pattern reveals the influence of all other waveguides in the array (see also Section 2 for more details about characteristics of conformal antennas vs. planar antennas).

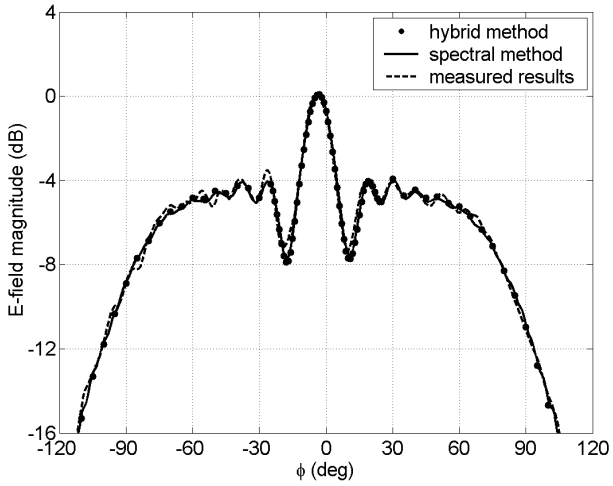

Figure 4-D. Embedded element pattern.

In order to additionally verify the results of the hybrid method we have defined the error of calculated S-parameters obtained by the hybrid method as:

$$\text{Error} = \frac{\left|S_{n,1}\right|_{HybridMethod} - \left|S_{n,1}\right|_{SpectralDomain}}{\left|S_{n,1}\right|_{SpectralDomain}} \tag{4.3}$$

The reference values are the results obtained with the program where no acceleration techniques are implemented.

The sensitivity of the error on the number of terms in the inverse Fourier series is shown in Fig. 4-E. Calculations were made for the array with the parameters described in the text above. Results show that there is almost no dependence on the number of modes used.

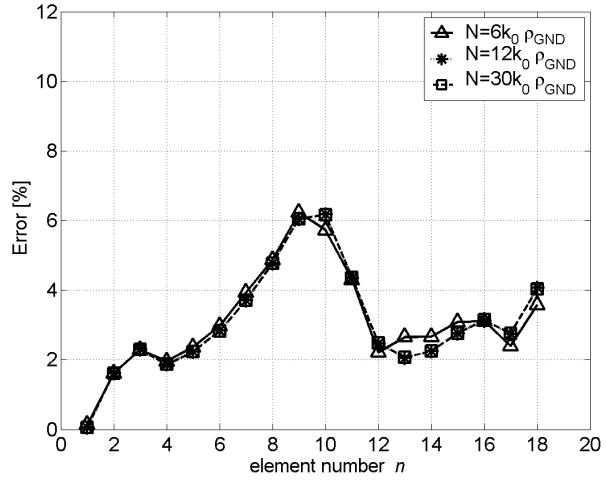

Figure 4-E. Sensitivity on number of terms *N* in the inverse Fourier series (k_0 is the wave number of free space, ρ_{GND} is the radius of the cylinder).

We have also varied the length of integration in the inverse Fourier transformation, and the results are shown in Fig. 4-G. It is important to mention that the spectral domain Green's function contain poles that correspond to the propagation constants of surface wave modes. These poles are located at the real k_z axis between k_0 and $k_n^{\max}$ ($k_n^{\max}$ is the maximum possible wave number) if the dielectric is lossless, and below the k_z axis if losses are present in the dielectric. In order to avoid numerical difficulties with the integration of Green's function around the poles, the path of integration used for calculating the inverse Fourier transformation in eq. (4.2) is moved from the poles as shown in Fig. 4-F. The parameter L_{int}, which we have varied in the calculations, is also shown in Fig. 4-F. The results in Fig. 4-G indicate that only a very short length of integration (L_{int} = 0) introduces a slight increase in the error. When the parameter L_{int} is larger than $5k_0$ there is no variation of the calculated results. Calculations were made for the array with the parameters described in the text above.

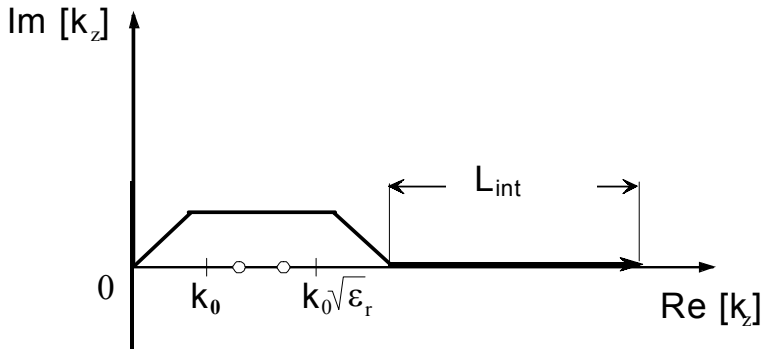

Figure 4-F. Path of integration used in calculations.

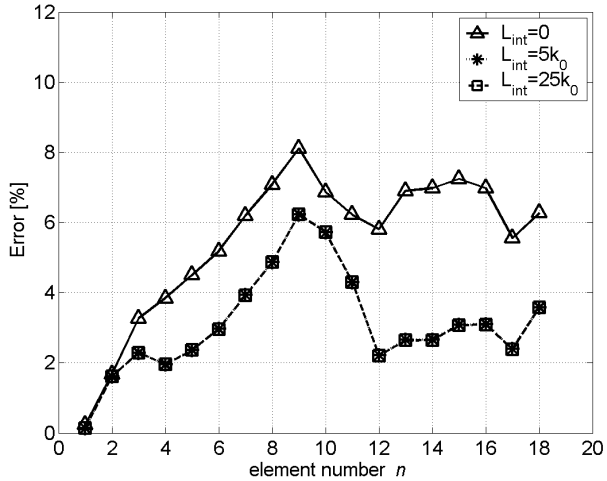

Figure 4-G. Sensitivity on length of integration in the inverse Fourier transformation.

Sensitivity of the error on permittivity of the dielectric cylinder is shown next in Fig. 4-H. Three values of permittivity were used in the calculations: (i) ε_r=1.1 (which is very similar to the permittivity of the air gap), (ii) ε_r=2.32 (the same value as for the radome in the experimental antenna), (iii) ε_r=4.0 (larger than in measurements). All other parameters of the array were the same as before (for example, the thickness of the air-gap was 0.085 cm). In all these cases the error is very small, and there is no significant increase of error for larger permittivity values.

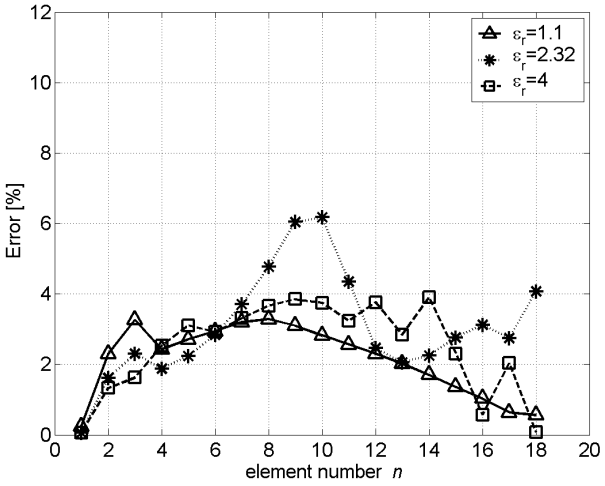

Figure 4-H. Sensitivity on dielectric permittivity.

However, in the case when ε_r=2.32 the error shows a rapid increase for centrally located elements which is not present in the other cases. This increase of error is a consequence of destructive interference of all coupling mechanisms, i.e. the coupling from the waveguide elements that are located around the considered pair of waveguides [6].

The influence of the thickness of the air-gap for three considered values of permittivity is analyzed in Fig. 4-I. Fig. 4-I-a shows sensitivity on the air gap thickness when dielectric cylinder with ε_r=1.1 is used. As expected, results are practically identical for various values of thickness since permittivity values of two dielectric layers are similar. Fig. 4-I-b. investigates the sensitivity on the air gap thickness when ε_r=2.32. Destructive interference as mentioned earlier is here clearly visible, and the error is increased when the thickness of the air gap is decreased. The third case, for which ε_r=4.0, shows a surprising result as seen in Fig. 4-I-c. The error is increased when the air-gap is increased. In other words, the error is bigger when the assumed homogeneous media, used for the calculation of the asymptotic part in eq. (4.2), is more similar to the actual media covering the cylinder.

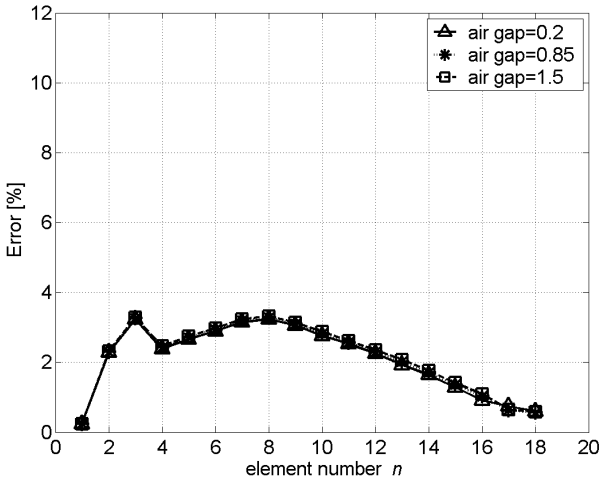

(a)

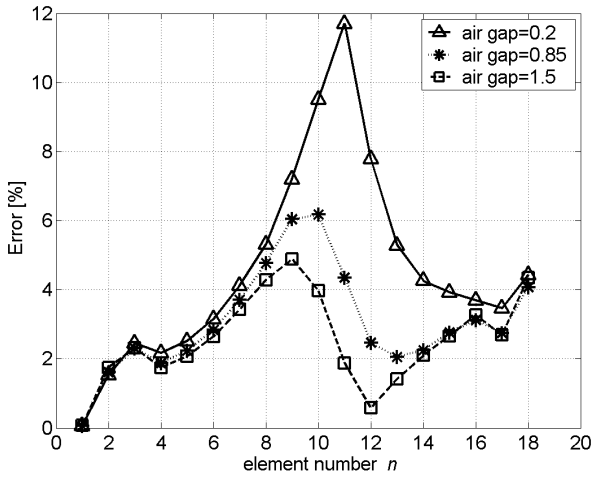

(b)

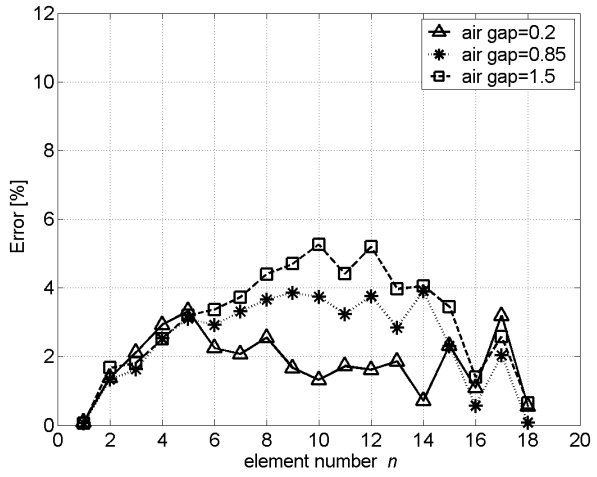

(c)

Figure 4-I. Sensitivity on air gap thickness for different permittivities.
(a) ε_r=1.1, (b) ε_r=2.32, (c) ε_r=4.0.

4.4 References

[1] R. F. Harrington, *Time-harmonic electro-magnetic waves*, McGraw-Hill, 1961.

[2] Z. Sipus, P.-S. Kildal, R. Leijon, and M. Johansson, "An algorithm for calculating Green's functions for planar, circular cylindrical and spherical multilayer substrates," *Applied Computational Electromagnetics Society Journal,* Vol. 13, No. 3., pp. 243-254, Nov. 1998.

[3] G.E. Stewart and K.E. Golden, "Mutual admittance for axial rectangular slots in a large conducting cylinder," *IEEE Trans. Antennas and Propagat.*, Vol. 19, pp. 120-122, Jan. 1971.

[4] A. Hessel and J.-C. Sureau, "Resonances in circular arrays with dielectric sheet covers," *IEEE Trans. Antennas and Propagat.*, Vol. 21, pp. 159-164, Mar. 1973.

[5] Q. Balzano, "Analysis of periodic array of waveguide apertures on conducting cylinders covered by a dielectric," *IEEE Trans. Antennas and Propagat.*, Vol. 22, pp. 25-34, Jan. 1974.

[6] Z. Sipus, M. Lanne and L. Josefsson, "Moment method analysis of circular cylindrical array of waveguide elements covered with a multilayer radome," *IEE Proc. Microwaves, Antennas & Propagtion,* vol. Feb. 2006.

[7] N. Kinayman and M.I. Aksun, "Comparative study of acceleration techniques for integrals and series in electromagnetic problems," Radio Science, Vol. 30, pp. 1713-1722, Nov.-Dec. 1995.

[8] K.Blagovic, I. Stevanovic, A.K. Skrivervik, "Convergence of infinite periodic Green's functions for the mixed potential integral equation," Proc. of ICECOM 2003, Dubrovnik, pp. 423-426.

[9] P.H. Pathak, N. Wang, W.D. Burnside and R.G. Kouyoumjian, "A uniform GTD solution for the radiation from sources on a convex surface," *IEEE Trans. Antennas and Propagat*., vol. 29, pp. 609-622, July 1981.

[10] P.H. Pathak and N. Wang, "Ray analysis of mutual coupling between antennas on a convex surface," *IEEE Trans. Antennas and Propagat.*, Vol. 36, pp. 911-922, Sept. 1988.

[11] P. Persson and L. Josefsson, "Calculating the mutual coupling between apertures on a convex circular cylinder using a hybrid UTD-MoM method," *IEEE Trans. Antennas Propagat.,* Vol. 49, pp. 672-679, Apr. 2001.

[12] P. Persson and R. G. Rojas, "High Frequency Approximation for Mutual Coupling Calculations Between Apertures on a PEC Circular Cylinder Covered with a Dielectric layer: Non-paraxial Region", *Radio Science*, vol. 38, August 2003.

[13] B. Thors and R. G. Rojas, "Uniform Asymptotic Solution for the Radiation from a Magnetic Source on a Large dielectric Coated Circular Cylinder", *Radio Science*, Vol.38, No.5, September 2003.

[14] McNamara D. A., C. W. I. Pistorius and J. A. G. Malherbe (1990), *Introduction to The Uniform Geometrical Theory of Diffraction*, Artech House, Boston, 1990.

[15] R.F. Harrington, *Field computation by moment method*, MacMillan, New York, 1968.

5 EDUCATIONAL ACTIVITIES

One of the activities that will help student exchange between various European academies and companies will be organization of the Ph.D. course on planar and conformal microstrip antennas. The course was originally planed for Autumn 2005, but due to some technical problems it is postpones to 2006. The course will hold at EPFL- Lausanne in February 2006.

This course will cover the theoretical aspect of the analysis and design of planar and conformal antennas. The first half of the course will deal with the fundamentals of the mathematical and electromagnetic models being used for the analysis of printed antennas. The static and quasistatic cases will be first discussed as a very useful introduction to the full-wave (dynamic) formulation. The second half will cover analysis methods for antennas embedded in multilayer structures of planar, circular cylindrical and spherical types, with real life applications.

The considered analysis of conformal antennas is based on using the moment method in the spectral domain. The Green's functions of the multilayer structure are constructed numerically by division in homogeneous subregions and using equivalence principle. The latter is a general approach applicable to multi-region problems of other kinds as well. Therefore, the course also gives an introduction to how general and complex structures can be divided in subregions that can be analyzed independently and efficiently by making use of the appropriate symmetries of each subregion. The lectures will therefore include definitions of different canonical structures with certain symmetries. For large structures the uniform geometrical theory of diffraction is an appropriate method. Antennas embedded in cylindrical structures of arbitrary cross section will also be treated.

The course will throughout contain examples of practical planar and conformal antennas and discussions of their application. The main focus of the lectures will be the structuring of the field problems into manageable sub-problems and presentation of results, rather than detailed mathematics.

The planned presenters of the conformal part of the course are Prof. Per-Simon Kildal (CHALMERS), Prof. Zvonimir Sipus (CHALMERS and University of Zagreb), Dr. Patrik Persson (KTH), and Dr. Silvia Raffaelli (Ericsson). The course will consist of lectures, self-study and assignments, and computer exercises. The course will have 5 credit units (5 ECU), and the assessment topology is: attendance 1 credit unit, assignments 1 credit unit, and computer exercise 3 credit units. The two weeks after the course should be allocated to solving computer exercise of 1-2 weeks duration. The exercises will be given out during the course and will normally involve some Matlab or Fortran programming. The developed program and verified results must be submitted within 4 weeks and be accepted to get 3 credit units.

6 FUTURE ACTIVITIES

The following actions are proposed for the project ACE-2:

- Full benchmarking of different conformal antennas and structures. The proposed validation cases are suitable for characterizing most-interesting types of conformal antennas. The participants will launch benchmarking simulations, and they will be compared with measurements. This activity will be done together with the activity 1.1 (modelling methods and software).

- Development of new hybrid programs that will result in programs set-up in common by several different groups, and which will have better/larger performances than original (already existing) software. In other words, the proposed activity will join research activities of different groups.

- Improvement of existing programs or development of new suitable numerical codes for an efficient analysis and synthesis of conformal antennas (e.g. extension of existing programs to be able to analyse large conformal arrays). The goal of the proposed activity is to structure research in direction of the most useful antenna architectures & geometries.

- Development of algorithms for beam synthesis and steering for conformal arrays. The conformal arrays with beamforming and beamsteering possibilities are still not fully explored, as well as algorithms for beam synthesis for conformal arrays. This is in particular important for future communication and radar systems.